THE ASTROPHYSICAL JOURNAL, 404:521–538, 1993 February 20

THE EVOLUTION OF GALAXIES IN RADIO-SELECTED GROUPS

JEREMY R. ALLINGTON-SMITH[1] AND RICHARD S. ELLIS[1]
Department of Physics, University of Durham, Durham DH1 3LE, United Kingdom
AND
ESTHER L. ZIRBEL[1] AND AUGUSTUS OEMLER, JR.[1]
Department of Astronomy, Yale University, New Haven, CT 06511
Received 1992 March 12; accepted 1992 August 31

ABSTRACT

In order to study the evolution of galaxies in small groups in a way unbiased by optical selection effects, we have observed the populations of galaxies around a sample of 98 strong radio galaxies, 65 with redshifts less than 0.25, and 33 with redshifts between 0.25 and 0.50. These radio galaxies were chosen to have the same range of radio power $10^{26} < P_{408} < 10^{28}$ W Hz^{-1}, at both high and low redshift. CCD photometry of fields containing the radio sources, and of nearby comparison fields, was obtained in the B and V bands for the low-redshift sample, and in the V and R bands for the high-redshift sample.

We have analyzed the properties of galaxies with $M_V \leq -19.0$ (assuming $H_0 = 50$ km s^{-1} Mpc^{-1} and $q_0 = 0.0$) within 0.5 Mpc of the radio galaxies, with the following results. (1) Strong radio galaxies occur in groups whose range of richness is broad, but not as broad as that of groups in general: radio galaxies may tend to avoid very poor groups. (2) There has been a slight decrease in the richness of radio groups since the epoch observed at $z = 0.4$, particularly among the FR II sources. (3) The luminosity function of the members of both high- and low-redshift radio groups is indistinguishable from that of nearby field galaxies. (4) Groups around nearby radio galaxies display the same relation between population and environment as do groups in general: richer groups contain redder galaxies. (5) However, groups at high redshifts show little indication of such a trend: groups of all richnesses have similar high fractions of blue galaxies. We conclude that galaxies in groups containing radio galaxies are typical of group members in general and are a good probe of the properties of normal galaxies. The difference between the properties of our low- and high-redshift samples suggests that *the morphology-environment relation is of recent origin and is steepening rapidly with time.* This steepening is most likely responsible for the rapid evolution previously observed in the colors of galaxies in rich clusters.

Subject headings: galaxies: evolution — galaxies: stellar content — radio continuum: galaxies

1. INTRODUCTION

The origin of the present forms and content of galaxies is a question of much interest, to which considerable attention, both observational and theoretical, has been devoted in recent years. Important clues may be obtained from the variation of galaxy properties with environment (Hubble 1936; Oemler 1974; Dressler 1980; Postman & Geller 1983), and, especially, from the variation of properties with epoch. It is well established that the stellar populations of many galaxies in the cores of rich clusters have evolved rapidly during recent times (Butcher & Oemler 1984a, hereafter B&O), becoming much redder, but the significance of this evolution for the general galaxy population is far from clear. The changes seen in clusters may exemplify those occurring everywhere and represent a general decline in the star formation rate in galaxies. Alternatively, they may be the result of processes peculiar to rich, dense clusters, and not of relevance to conditions elsewhere.

The most straightforward way to resolve this question is to observe galaxies as a function of lookback time in the general field, but this is considerably more difficult than observations of cluster galaxies, because the redshift of each member of a statistically significant field sample must be carefully compiled with due attention to completeness. Attempts to circumvent this difficulty by using the information contained in deep counts of galaxies as a function of brightness and color have suggested substantial evolution in the luminosities and colors of the bulk galaxy population (Bruzual & Kron 1980; Koo 1986; Tyson 1988). However, recent spectroscopic surveys (Broadhurst, Ellis, & Shanks 1988; Colless et al. 1990) reveal a more complex situation, suggesting that the inferred changes may be due primarily to the evolution of nearby low-luminosity galaxies.

Such field samples are ideally complemented by observations of small groups of galaxies. The environment in such systems is more similar to that of the field than to that in rich clusters, and one would not expect processes peculiar to rich clusters to operate with much effectiveness in groups. Groups, therefore, probe environments like the field with many of the same economies of observation afforded by rich clusters. Furthermore, if it is established that field and cluster galaxies do evolve in different ways, groups will allow us to bridge the two environmental extremes and, perhaps, understand why they differ.

Unfortunately, poor groups cannot be seen easily at even moderate redshifts, because their contrast against the background is weak. Thus, any attempt to construct a catalog of high-redshift groups from the inspection of the distribution of galaxies on the sky would result in a sample which was highly contaminated by random surface density fluctuations which were not real physical associations. Nevertheless, many galaxies are members of groups. If one could assemble, for

[1] Visiting Astronomer, Kitt Peak National Observatory, National Optical Astronomy Observatories. NOAO is operated by the Association of Universities for Research in Astronomy, under contract for the National Science Foundation.

example, a sample of luminous elliptical galaxies of known redshift, one would expect to find a statistical excess of galaxies at small projected distances on the sky from the luminous ellipticals, which would be physically associated with the latter objects.

Studies of radio galaxies provide us with the means of assembling such a list. It is known that most strong radio galaxies are luminous ellipticals and that they often occur in groups (e.g., Prestage & Peacock 1988, 1989). Many are now known at quite high redshift. If we can demonstrate that the groups of galaxies found by such a procedure contain galaxies of normal properties, unaffected by the phenomena which gave rise to the radio galaxy, we can use them to probe the evolution of galaxies in low-density regions to quite high redshift. In this paper we present the first results of such a study. We have obtained photometry of the environments of 98 radio galaxies with redshifts between 0.0 and 0.5. These galaxies were selected to produce a sample of objects which is as homogeneous as possible. This paper describes the sample and the observations of it, and uses the distribution of the colors of the galaxies surrounding the radio galaxies to study the properties of the galaxy population as a function of redshift. These data also have much to say about the radio galaxies themselves and their relation to their environments. An analysis of these aspects will be the subject of future papers.

2. OBSERVATIONS

2.1. *Choice of Sample*

Because our goal is to address the evolution of group properties with look-back time, it is important to adopt selection criteria which are as independent of redshift as possible. Only in this way can the contamination biases that have plagued earlier studies be minimized. The strategy we explore in this paper is the selection of groups according to the presence of a radio galaxy. Possible properties of the radio galaxies that we could use include radio luminosity, spectral index, and radio morphology. A priori it is not clear to what extent selecting by any of these observables might influence a group catalog. However, because we are primarily concerned *with the evolutionary properties of the associated galaxies*, selecting by radio power has the important advantage of being independent of those passbands we will use to measure the evolution. Although there will be redshift-dependent luminosity biases in any flux-limited samples, these can be minimized by selecting from the same parts of the radio luminosity function. Only strong evolution of the radio luminosity function would then distort our sample, and we can check for such behavior directly.

We cover the redshift range from 0.0 to 0.5, in two samples, a low-redshift sample with $0.0 < z < 0.25$, and a high-redshift sample with $0.25 < z < 0.5$. Given existing catalogs of radio galaxies, this is best accomplished by selecting sources whose mean radio power at 408 MHz, P_{408}, is close to 10^{27} W Hz^{-1} (assuming $H_0 = 50$ km s^{-1} Mpc^{-1}, and $q_0 = 0.0$), i.e., above the break in the radio luminosity function. These are strong radio sources, and the majority are of Fanaroff-Riley class II. We have included only radio galaxies with spectroscopically determined redshifts, since the uncertainties in estimating redshifts from optical photometry are unacceptably large for our purposes. Radio galaxies were selected from the following: the 3CR samples of Laing, Riley, & Longair (1983) and Spinrad et al. (1985, augmented with private communications from H. Spinrad), the "1 jansky" sample of Allington-Smith et al. (1988), the 5C12 sample of Benn et al. (1988) and G. Rixon (private communication), and the 5C6 sample of Perryman, Downes, & Lilly (1985). In addition, radio galaxies were selected from the compilation of Burbidge & Crowne (1979). This added a number of other B2, Parkes, 4C, and 5C sources to our sample. Two sources whose radio powers are much below our lower flux limit, 5C 3.100 and 5C 3.175, were mistakenly included because the radio fluxes for 5C3 sources quoted in Burbidge & Crowne are too high by a factor of 100. We shall demonstrate later that their inclusion does not affect our conclusions.

It is advantageous to know the radio morphologies of our sample. These were obtained from the literature, and, in the case of 4C 29.44, from a new observation with the Cambridge 5 km telescope, at 2.7 GHz, for which we are indebted to G. Pooley. In many cases, the Fanaroff-Riley class was estimated directly from the maps presented using Fanaroff & Riley's (1974) classification procedure. For many of the low-redshift sample, no radio morphological information was available. From their radio luminosities, one might expect most of these to be of Fanaroff-Riley class II, but we prefer not to make that prejudgment. Spectral index information was taken from the literature, except for three low-redshift sources for which an index of 0.75 was assumed.

Information on those radio galaxies for which useful photometry was obtained, 65 in the low-redshift sample and 33 in the high-redshift sample, is presented in Tables 1 and 2. The first five columns contain the source's IAU designation, its more common name (where available), the redshift, logarithm of the radio power (W Hz^{-1} at 408 MHz), and FR type ("C" denotes compact structure). Figure 1 plots radio power versus redshift in our sample and demonstrates the extent of our success in obtaining a homogeneous sample. Although there is a clear increase in radio power with redshift, the mean power of the two samples differ by a factor of only 4, which is much less than the overlap. As an illustration of the difficulties, the solid line represents the limit of the 3C sample ($S_{178} = 10$ Jy), trans-

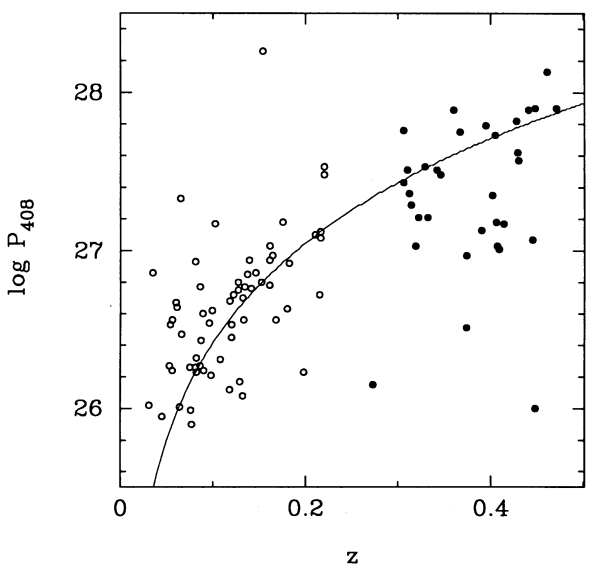

FIG. 1.—Radio power vs. redshift for the entire sample. *Open circles:* low-redshift sample; *filled circles:* high-redshift sample. The line represents the approximate limit of the 3C catalog.

TABLE 1

THE LOW-REDSHIFT SAMPLE

IAU	Other	z	log P	FR	$N_{0.5}^{-19}$	f_B	Notes	IAU	Other	z	log P	FR	$N_{0.5}^{-19}$	f_B	Notes
0034-014	3C15	0.073	26.35	I	3.5±3.8		2	1123+203	4C20.25	0.132	26.08		1.0±1.3		1,2
0035-024	3C17	0.220	27.48	II	9.4±4.3	0.32±0.22	1	1214+038	PKS	0.077	25.9		14.5±5.7	0.08±0.18	2,3
0039+400	5C3.100	0.071	24.02		3.9±3.6			1215+039	PKS	0.075	26.26	I	22.2±7.1	0.08±0.13	2,3
0043-424	PKS	0.053	26.27	II	-2.1±3.6			1216-100	PKS	0.067	26.43		8.7±3.8		1
0044+398	5C3.175	0.134	24.46		13.8±5.0	0.14±0.25		1239+025	4C02.39	0.180	26.63		9.3±3.4		1
0051-038	3C26	0.210	27.10		-1.9±3.6			1251+278	3C277.3	0.086	26.27	II	-0.4±4.1		
0055-016	3C29	0.045	25.95	I	4.6±2.5		2	1330+022	3C287.1	0.216	27.08	II	2.0±2.6		1
0106+130	3C33	0.060	26.67	II	6.3±4.2	0.19±0.20		1331-099	PKS	0.081	26.26	II	2.8±1.8		1
0114-476	PKS	0.146	26.86	II	0.0±4.7			1340+053	4C05.57	0.133	26.56		3.6±1.8		1
0214-480	PKS	0.064	26.01	I	9.8±6.1	0.30±0.20	2	1345+123	4C12.50	0.122	26.72		-0.4±3.3		1
0218-021	3C63	0.175	27.18	II	11.6±4.3	0.46±0.54		1417-192	PKS	0.120	26.45		4.0±5.6		1
0303+390	4C39.11	0.161	26.78		3.5±4.8			1441+522	3C303	0.141	26.76	II	7.8±2.9	0.50±0.22	
0331-013	3C89	0.139	26.94	I	15.9±5.5	0.21±0.11		1502+262	3C310	0.054	26.53	II	12.2±4.5	-0.07±0.36	
0349-278	PKS	0.066	26.47	II	11.8±4.7	0.10±0.21	2	1510+709	3C314.1	0.120	26.53	I	1.6±3.0		
0356+102	3C98	0.031	26.02	II	3.4±2.4		2	1529+242	3C321	0.096	26.54	II	-0.7±3.7		1,2
0404+035	3C105	0.089	26.60	II	14.6±5.1		1	1549+202	3C326	0.090	26.24	II	3.9±3.8		1,2
0456-043	4C-04.17	0.118	26.12		-3.2±4.2			1615+324	3C332	0.152	26.80	II	6.2±4.2	0.09±0.22	
0511+048	3C135	0.127	26.80		-6.7±5.6			1641+173	3C346	0.161	26.94	I	10.0±4.6		1
0518-458	PKS	0.035	26.86	II	0.2±2.9		2	1648+050	3C348	0.154	28.26	I	31.6±7.4	-0.06±0.11	
0521-365	PKS	0.061	26.64	I	1.4±3.4			1832+474	3C381	0.161	27.03	II	8.5±5.3	0.70±0.26	
0604-203	PKS	0.164	26.97		-2.1±1.4		1	1845+797	3C390.3	0.056	26.56	II	14.5±4.9	0.30±0.22	
0719-553	PKS	0.216	27.12		7.0±5.0	0.28±0.37		1928-340	PKS	0.098	26.21	II	29.1±8.5	0.16±0.14	
0734+805	3C184.1	0.118	26.68	II	2.3±4.2			1934-638	PKS	0.182	26.92		-1.1±6.9		
0812-029	3C196.1	0.198	26.23		11.8±4.6		1	2030-230	PKS	0.132	26.70		8.9±4.6	-0.21±0.36	
0819+061	3C198	0.082	26.23	II	10.7±4.3		1,2	2045+068	3C424	0.127	26.75	I	17.8±5.7	0.18±0.12	
0915-118	3C218	0.065	27.33	I	31.0±5.5	0.13±0.06		2121+248	3C433	0.102	27.17	I	12.6±4.7	0.04±0.23	
0936+361	3C223	0.137	26.85	II	0.8±4.7			2130-538	PKS	0.076	25.99		18.4±5.8	0.22±0.13	2
0938+399	3C223.1	0.108	26.31	II	2.7±3.2			2221-023	3C445	0.056	26.24	II	4.5±2.4		
0939+141	3C225a	0.134	26.77		0.8±3.2			2243+394	3C452	0.081	26.93	I	18.2±5.5	0.45±0.14	
0945+076	3C227	0.086	26.77	II	4.3±4.1			2300-189	PKS	0.129	26.17	I	-1.7±5.0		
1000+201	4C20.20	0.168	26.56	I	7.1±5.0		1	2314+038	3C459	0.220	27.53	II	2.6±2.5		
1003+351	3C236	0.099	26.62	II	-0.8±2.5			2322-123	PKS	0.082	26.32		16.8±5.6	0.08±0.12	2
1007+142	4C14.36	0.215	26.72		0.7±2.0		1								

NOTES.—(1) Unreliable colors. (2) Small area photometered. Corrections applied to $N_{0.5}^{-19}$ and f_B. (3) Internal zero point. See text.

TABLE 2

THE HIGH-REDSHIFT SAMPLE

IAU	Other	z	log P	FR	$N_{0.5}^{-19}$	f_B	IAU	Other	z	log P	FR	$N_{0.5}^{-19}$	f_B
0035+13	3C16	0.405	27.73	II	13.2±6.1	0.68±0.28	1358+62	4C62.22	0.429	27.62	C	9.1±5.4[a]	0.13±0.44
0101+023	PKS	0.390	27.13	II	15.2±5.8	0.13±0.20	1419+42	3C299	0.367	27.75	II	8.4±5.3	0.14±0.38
0126+29	3C42	0.395	27.79	II	-4.1±4.0		1452-04	3C306.1	0.441	27.89	II	8.8±5.3	0.45±0.35
0213+33	5C6.142	0.448	26.00	II	23.3±7.2	0.22±0.15	1508+08	3C313	0.461	28.13	II	11.6±8.3[a]	
0221+28	3C67	0.310	27.51	II	-1.9±5.3		1530+36	3C320	0.342	27.51	II	17.2±6.4	0.13±0.18
0229+034	PKS	0.273	26.15	II	3.5±4.3		1539+34	4C34.42	0.402	27.35	II	1.5±5.2	
0337-216	PKS	0.414	27.17		2.7±4.5		1603+32	B2	0.374	26.51		4.1±5.0	
0411+11	3C109	0.306	27.76	II	2.0±5.3		1626+28	3C341	0.448	27.90	II	9.9±6.2	0.21±0.31
0822+34	B2	0.406	27.18	II	0.6±4.5[a]		1645+17	4C17.71	0.314	27.29		-4.7±5.1	
0847+37	B2	0.407	27.03	II	7.3±6.6[a]		2121+16	3C434	0.322	27.21	II	10.4±7.3	-0.91±1.04
1025+39	B2	0.36	27.89	II	7.2±5.0	0.05±0.49	2126+07	3C435	0.471	27.90	II	33.5±8.1	0.21±0.13
1107+379	4C37.29	0.346	27.48	II	15.1±5.2	0.11±0.16	2152-218	PKS	0.306	27.43	C	0.5±5.0	
1134+015	4C01.31	0.43	27.57		0.0±4.8[a]		2159-187	PKS	0.332	27.21		0.4±5.9	
1152+30	4C29.44	0.329	27.53	II	70.4±9.1	0.10±0.05	2309+18	3C457	0.428	27.82	II	10.3±5.8	0.13±0.27
1201+39	B2	0.445	27.07	II	6.7±5.2	0.49±0.43	2322+22	4C27.51	0.319	27.03		21.0±6.8	0.51±0.16
1245+34	B2	0.409	27.01	II	14.9±6.4[a]	0.75±0.16	2347+302	B2	0.374	26.97		6.2±4.9	0.48±0.37
1303+369	5C12.251	0.312	27.36		36.3±7.2	0.22±0.10							

[a] Significant correction needed to −19. completeness limit.

formed to 408 MHz via a spectral index of 0.75. The majority of sources in the 3C catalog crowd to the top side of this line.

2.2. *Photometry*

Our strategy in studying galaxy evolution in the ratio groups will be to obtain rest frame $B-V$ colors for all galaxies brighter than $M_V = -19.0$ within 0.5 Mpc radius of the radio galaxy. To do this, we have obtained CCD observations of the low-redshift sample in the B and V bands and observations of the high-redshift sample in the V and R bands, as defined by the Mould filter set. At redshifts of about 0.4, the latter bands approximate the rest frame B and V bands, so that we sample similar portions of the rest frame spectral energy distribution in our low-and high-redshift samples. This enables us to transform our data to the rest frame with minimal model dependence. Observations were made over the period 1986 through 1989, using telescopes at the Kitt Peak National Observatory, Cerro Tololo Interamerican Observatory, and the Observatorio del Roque de Los Muchachos on La Palma. The observations are summarized in Table 3.

Observations of each radio source consisted of one or more fields centered on the radio galaxy and one or two fields, typically offset by about 20′ (and never less than 15′) to provide estimates of field galaxy and stellar contamination. If the radio source was of too low a redshift for the CCD to cover the entire central 0.5 Mpc radius area, a mosaic of four fields was usually constructed. Each field was typically observed for several frames in each band. Total exposure times were adjusted to produce colors of adequate accuracy ($\sigma \approx 0.15$ mag) at $M_V = -19.0$. Photometric zero points and color transformations were defined using observations of standard stars. During the first observing runs these consisted of Landolt standards (Landolt 1973, 1983) and CCD standard fields from Christian et al. (1985); subsequent runs used only Landolt stars and Graham (1981) E region standards. Photometry was reduced to the Johnson B and V bands and the Kron-Cousins R band, as defined by the standard stars. Those observations affected by instrumental problems or nonphotometric conditions and those fields thought to be affected by large and poorly determined Galactic extinction are noted in Table 1. The photometry derived from these questionable data is adequate for determining group membership properties, but we have excluded it from our analysis of galaxy colors.

Photometry of the low-redshift sample was reduced at Yale, using a suite of programs developed over the past 20 years to perform automatic galaxy photometry. Photometry of the high-redshift sample was reduced at Durham, using the Starlink Figaro package. In both cases, the procedure was as follows. After bias subtraction and division by dome flats, the frames were flattened again by mode-fitting to the sky. All objects consisting of at least $n_{\min}$ pixels above a specified surface brightness threshold were cataloged and isophotal magnitudes calculated. The value of $n_{\min}$ was varied with the CCD pixel scale in each data set, to establish a minimum object size of about 2 arcsec^2. Objects smaller than this were almost always found to be CCD defects or cosmic ray events. The surface brightness threshold was set to twice the standard deviation of the sky noise in each frame, and therefore varies with the data quality, but is typically a few percent of sky.

The inclusion of stars in our analysis will not introduce systematic errors since, on average, equal numbers of stars will occur in the group and field (offset) frames. However, their inclusion will lead to an increase in the random errors. Although the ratio of stars to galaxies is typically only 1 to 4 in the high-redshift groups, the ratio may be as high as 5 to 1 in extreme cases in our low-redshift data set. We have therefore attempted to separate stars from galaxies using a classification parameter derived from the curve of growth of the object image. Marginal objects, and objects too faint to classify in this manner were considered to be of unknown type, and were included with the galaxies in all subsequent analysis. For a few high-redshift fields, we have not been able to separate stars from galaxies because the stellar locus could not be established unambiguously.

It is important to check that we have not systematically misclassified galaxies as stars since this could lead to an underestimate of the numbers of galaxies in the groups. For our high-redshift data, where the star/galaxy separation is hardest because of the paucity of objects to define the stellar locus, we find that the surface density of objects classified as stars in the field frames is identical to the density in the group frames even though the number of galaxies is 60% higher in the group frames. Therefore, we conclude that this source of bias is negligible. Figure 2 shows the surface density, ρ, of objects classified as stars or galaxies in the high-redshift field frames as a function of V magnitude. The best fit to the galaxy data for $V < 22$ has a slope $d \log \rho/dV = 0.44$ which is typical of galaxy counts in similar passbands (e.g., Kron 1980). Fainter than $V = 22$, the galaxy counts deviate slightly from the straight line until the data start to become incomplete at $V \sim 23$. This suggests that the star/galaxy separation is quite reliable even at $V = 22$.

Our galaxy search routine yields isophotal magnitudes for each object. However, accurate colors can be obtained only from photometry within an aperture which is the same in both passbands. The area chosen for this aperture is based on the size of the galaxy within the limiting isophote as seen in the redder passband. This area varies with isophotal magnitude in a characteristic way, a typical example of which is shown in

TABLE 3

OBSERVING CONFIGURATIONS

Sample	Telescope	CCD	Image Scale (arcsec pixel^{-1})	Array Size	Field Size
Low-redshift	KPNO 0.9 m	TI	0.86	396 × 396	5.7 × 5.7
	CTIO 0.9 m	TI	0.50	396 × 396	3.3 × 3.3
		RCA	0.50	316 × 508	2.6 × 4.2
High-redshift.....	La Palma 4.2 m	EEV	0.54	370 × 380	5.7 × 5.7
	La Palma 2.5 m	RCA	0.74	316 × 508	3.9 × 6.3
	KPNO 4.0 m	TI	0.58	396 × 396	3.8 × 3.8
	KPNO 2.1 m	RCA	0.38	316 × 508	2.0 × 3.2
		TEK	0.34	508 × 508	2.9 × 2.9

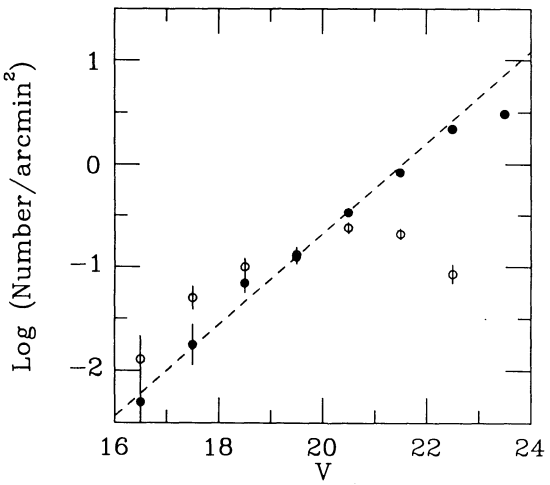

FIG. 2.—Surface density as a function of V magnitude of objects found in field (offset) frames in the high-redshift sample. *Open circles:* stars; *filled circles:* galaxies; *dashed line:* the slope of the differential galaxy counts in F of Kron (1980).

Figure 3*a*. Well above the limiting magnitude of the CCD frame, the area is an exponential function of the isophotal magnitude. A circular aperture of equal area would have a radius

$$r_{ap} = r_0\, 10^{-\beta(m_{iso}-m_0)} . \quad (1)$$

Typical values of the parameters are $r_0 = 2''.5$, $m_0 = 21.5$, $\beta = 0.15$.

We have defined two aperture magnitudes for each object, measured within circular apertures of radii $r_1 = r_{ap}/2^{1/2}$ and $r_2 = (2)^{1/2} r_{ap}$. Fainter than some magnitude we hold r_{ap} constant so that the smaller aperture r_1 never falls below $\sim 1''.5$. The variation of r_1 and r_2 with magnitude is shown in Figure 3*a*. We calculate colors using aperture r_1 since this gives the optimum signal-to-noise ratio. However, r_1 can be quite small for the fainter objects, and it is possible for differences in seeing or focus between frames to produce systematic errors in the measured colors. To test for this, we compare the colors determined within r_1 with those determined within r_2. The latter have greater uncertainty due to the increased sky area sampled but should be much less sensitive to systematic errors. In those few cases where systematic offsets were found, the colors derived from r_1 were corrected for this offset. Magnitudes were determined with r_2 since this samples a substantial fraction of each object's light. In fact, surface photometry of a sample of galaxies in many fields shows that this aperture magnitude is fainter than the total magnitude by an average of 0.2 mag and is therefore similar to the isophotal magnitudes of Shanks et al. (1984) and the isophote-based aperture magnitudes of Kirshner et al. (1983).

We can assess the competeness of our catalogs from both internal and external considerations. In Figure 3*b* we present for the same data set discussed above, the isophotal area versus aperture magnitude calculated within r_2. As expected, the plot is similar to Figure 3*a* because, for faint sources, aperture magnitudes are, statistically, similar to isophotal ones. It is seen that the relationship becomes steep as galaxies approach a limiting magnitude. The completeness limit is thus internally defined when the isophotal area in pixel units reaches the threshold value, n_{min}, indicated by the vertical line. The galaxy counts shown above in Figure 2 provide similar completeness limits, consistent with those determined by this method.

As an external check on possible incompleteness introduced by our search algorithm, we have run the Yale-based software on the standard PDS image of a deep 4 m b_j prime focus plate discussed by Koo, Ellis, & Windhorst (1989). This image has been the subject of a detailed comparative study by various groups worldwide. Although a photographic image, the sky

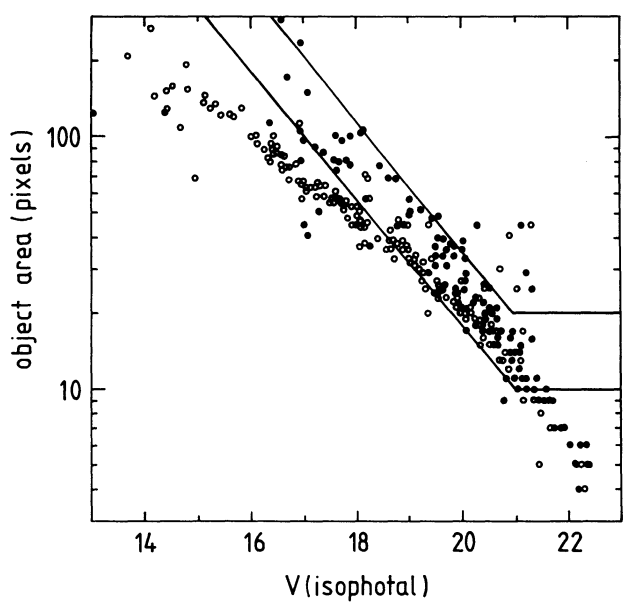

FIG. 3*a*

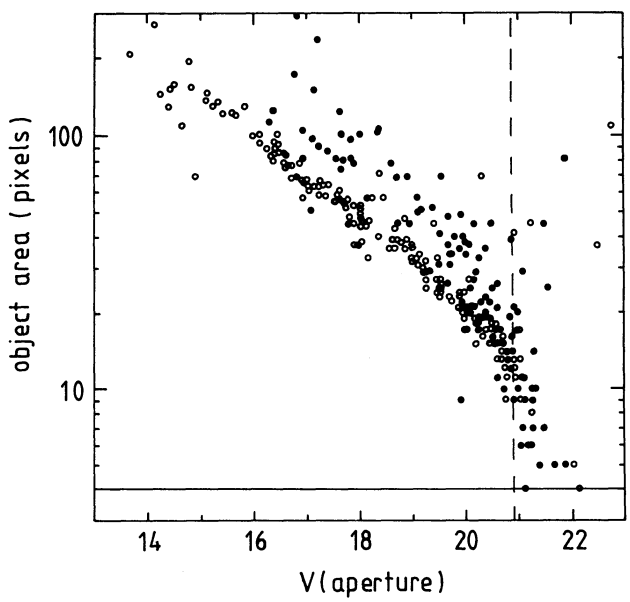

FIG. 3*b*

FIG. 3.—Object size vs. magnitude in a typical low-redshift field. *Filled circles:* galaxies; *open circles:* stars. (*a*) Size vs. isophotal magnitude. The solid lines are the sizes of the two photometry apertures used. (*b*) Size vs. aperture magnitude. The horizontal line is the limiting object size, n_{lim}; the vertical dashed line is the completeness limit of the data.

signal-to-noise ratio is inferior to our CCD data and thus provides a more stringent test. As discussed by Koo, Ellis, & Windhorst, a master catalog is created by comparing the detections made across all group catalogs. Deeper Hale 5 m Four-Shooter CCD data are available for a subset of the prime focus field and a comparison with the master catalog shows the latter to be a highly reliable source with which to compare individual group catalogs. Ninety percent of the master list was found by the Yale software indicating excellent completeness to an average depth of $b_J \simeq 24.1$.

The foregoing has demonstrated the consistency of our magnitude system and the completeness of the data. There are, in addition, several internal and external checks by which we may estimate their random errors. We may calculate the expected errors in magnitudes and colors of objects due to photon and readout noise. The estimated color errors range from less than 0.01 mag for the brightest objects to about 0.15 mag for objects near the limit of completeness. These error estimates can be compared with the scatter between the values obtained from independent pairs of frames. This comparison shows that the internal error estimates are accurate predictors of the true errors of all but the brightest galaxies, whose scatter does not approach zero as predicted by the formal error estimates. This is to be expected, since there are other sources of error, such as centering differences, errors in flat-fielding, etc, which are less magnitude dependent.

Totally external checks on the quality of our photometry can be made by comparing our photometry of the radio galaxies with the published work of Sandage (1972b, 1973a), and Smith (1989). Figures 4 and 5 compare their magnitude and color measurements with ours. It is apparent from Figure 4 that there is a difference in magnitude zero points of about 0.02 mag. The scatter in aperture magnitude differences decreases substantially for larger apertures, suggesting that much of the scatter is due to aperture centering problems or to seeing differences, rather than to intrinsic errors in the photometry. Figure 5 compares our colors for the individual galaxies with the mean of the measurements of Sandage and Smith. The open circle is 3C 433. We are suspicious of the Sandage $B-V$ color, which is due to a single measurement, and which is not consistent with the quoted $U-B$ color. Ignoring 3C 433, we find an offset of our colors relative to those of Sandage + Smith of only 0.03 ± 0.015. From the scatter between the two authors, we estimate the error in the averaged Sandage + Smith colors to be about 0.06 mag. The scatter in Figure 4 ($\sigma = 0.078$) then implies an rms error in our photometry of 0.05. This is consistent with that estimated from the comparison of frame pairs described above and implies that we can accurately estimate the color errors for the fainter galaxies if we add in quadrature to our formal error an additional error of 0.045 mag. The latter accounts for all sources of error other than photon noise. Our final conclusion is that our total random color errors are always < 0.15 mag.

3. DATA ANALYSIS

3.1. *Reduction to the Rest Frame*

The goal of this study is to search for evolution in the stellar populations of the galaxies in our sample. Following B&O, we do this by measuring changes in the rest frame colors of galaxies relative to those of early-type galaxies at the same epoch. Because galaxy populations vary with environment and galaxy luminosity, we need to define a uniform sample of galaxies in

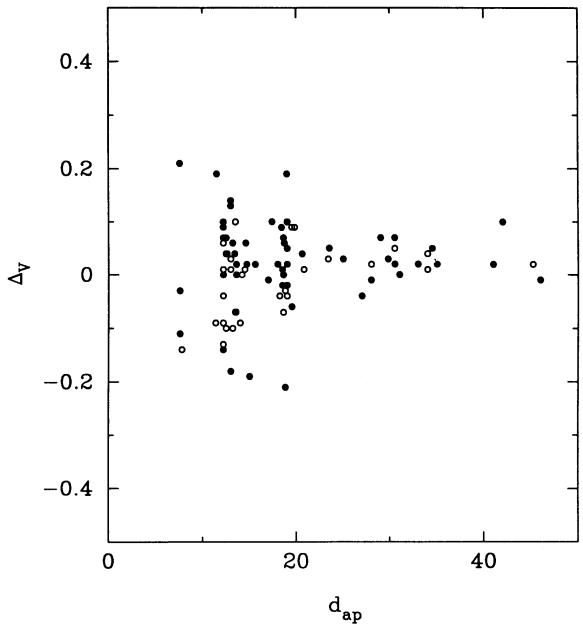

FIG. 4.—Differences in aperture magnitudes between our photometry and that of Sandage (*filled circles*) and Smith (*open circles*), plotted vs. the diameter of the aperture.

all groups, independent of redshift. Balancing a number of considerations including observing efficiency, backgound contamination, and the need for samples which are of adequate size and which typify the galaxy content of the groups, we have chosen to define a sample consisting of objects whose absolute V magnitudes, $M_V \leq -19.0$, and whose projected distances from the radio galaxy are less than 500 kpc. Such an area would be rather small for the study of rich clusters, but should be well matched to the sizes of the poor groups which we expect to predominate in this survey. The dependence on q_0 is not great at these redshifts. We assume $q_0 = 0.0$; the effect on the results of choosing a different value is discussed later. Of greater concern is the possibility of luminosity evolution in the galaxies. To avoid any assumptions about the amount of such evolution, we shall approach the problem in a semiempirical

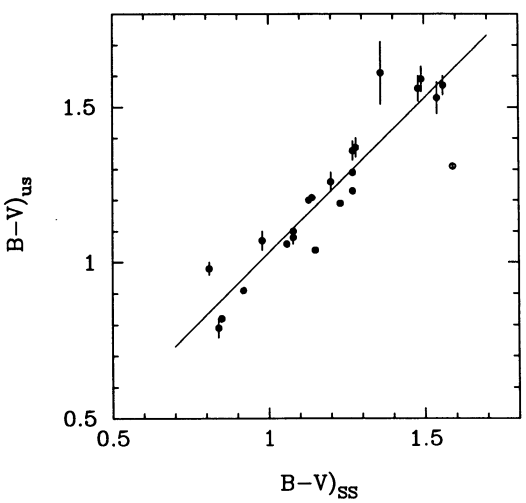

FIG. 5.—Our $B-V$ colors of radio galaxies vs. those of Sandage and Smith. The open circle is Sandage's color for 3C 433 (see text).

manner, using photometry of the brightest members of rich clusters (BCMs) to define the expected colors, $C_E(z)$, and apparent magnitudes, $m_E(z)$, of bright ellipticals in our observed bands at the redshifts of our radio groups.

For the low-redshift sample, whose photometry is in the B and V bands, we use the magnitude-redshift (m-z) relation for brightest cluster members, measured within Sandage's metric diameter of 86 kpc, as defined by the photometry of Sandage (1972a, 1973a, b), Sandage, Kristian, & Westphal (1976), and Kristian, Sandage, & Westphal (1978) to specify, at every redshift, $V_E(z, M_V^{BCM})$, the apparent V magnitude of elliptical galaxies of absolute magnitude $M_V^{BCM} = -23.30$. With suitable normalization of the magnitudes, these data are well fitted by the $m - z$ relations derived by Pence (1976) and Guiderdoni & Rocca-Volmerange (1988). The Pence relation uses only the k-corrections calculated from nearby ellipticals, while the latter prediction is based on a full evolutionary model of ellipticals. Their similarity is due to the minimal evolution expected over the range of redshifts observed in the low-redshift sample.

For the high-redshift sample, we determine the R-band m-z relation in a similar way, using Johnson R (R_J) photometry from the same sources, transformed to Kron-Cousins R (R_{KC}). The resulting Hubble diagram is presented in Figure 6*a*. Unfortunately, at redshifts greater than 0.3 there is insufficient published BCM photometry to adequately define the m-z relation. We have, therefore, supplemented these data with the m-z relation defined by FR II radio galaxies, whose suitability for this purpose can be justified a posteriori. We use the photometry of Sandage (1972b, 1973b), and we also determine R magnitudes within 86 kpc apertures for the FR II radio galaxies in our dataset. The resulting Hubble diagram is presented in Figure 6*b*. The m-z relation is almost as tight as that for BCMs but is, at every z, fainter than the latter. In Figure 6*c* we shift the FR II line by $\Delta R = -0.60$ mag to best align it with that of the cluster BCMs. The shifted m-z relations appear to be completely consistent with each other, in both scatter and slope. We therefore put a smooth curve through the combined data, and take this line to define $R_E(z, M_V^{BCM})$, the expected locus of ellipticals with absolute magnitudes $M_V = M_V^{BCM}$.

A similar approach can be applied to the galaxy colors. B&O avoided the need for an absolute color calibration by measuring, in the color-magnitude plot of rich clusters, the distribution of galaxy colors relative to the locus of early-type galaxies. Such an approach was satisfactory because that locus is well defined in rich clusters: early-type galaxies at redshifts less than $z \approx 0.7$ have a narrow dispersion of colors about the expected color-magnitude line. However, most of our groups are too poor to determine such a locus. Instead, we use Sandage's BCM photometry, suitably transformed, to define $C_E(z, M_V^{BCM})$, the expected $B-V$ and $V-R$ colors versus redshift for elliptical galaxies of $M_V = M_V^{BCM}$. In addition to transforming R_J to R_{KC}, a further transformation is needed because the bands of the CCD photometry do not correspond exactly to the photoelectric BVR bands. As part of the reduction process, our photometry has been transformed to the photoelectric bands using observations of standard stars, but the relation between the bands differs for stars and zero-redshift galaxies, on the one hand, and for redshifted galaxies on the other. The size of this effect has been determined from synthetic colors calculated using Pence's (1976) spectral energy distributions for normal galaxies; it can be as large as 0.20 mag at $z = 0.40$.

We use Visvanathan & Sandage's (1977) determination of the color-magnitude relation as a function of wavelength to establish $\partial C_E/\partial m$, the slope of the early-type galaxy locus in our observed color bands, for galaxies at each redshift. Corrections for reddening within our own Galaxy are applied using the Burstein & Heiles (1982) model for Galactic extinction. With the expected locus of elliptical galaxies defined, we can measure ΔC, the difference between C_{gal}, the observed color of each galaxy and that of the elliptical locus at the same absolute magnitude. We convert to differences in the restframe $B-V$ colors, $\Delta(B-V)_0$, using values of $\partial(B-V)_0/\partial C$ calculated at each redshift from Pence's spectral energy distributions. Finally, we used the same spectral energy distributions to determine $\partial M_V/\partial C$, the variation with color in the absolute V magnitude at a given apparent magnitude. To summarize,

$$\Delta(B-V)_0 = \frac{\partial(B-V)_0}{\partial C}\left\{C_{gal} - C_E(z, M_V^{BCM}) + \frac{\partial C_E}{\partial m}\left[m - m_E(z, M_V^{BCM})\right]\right\} \quad (2)$$

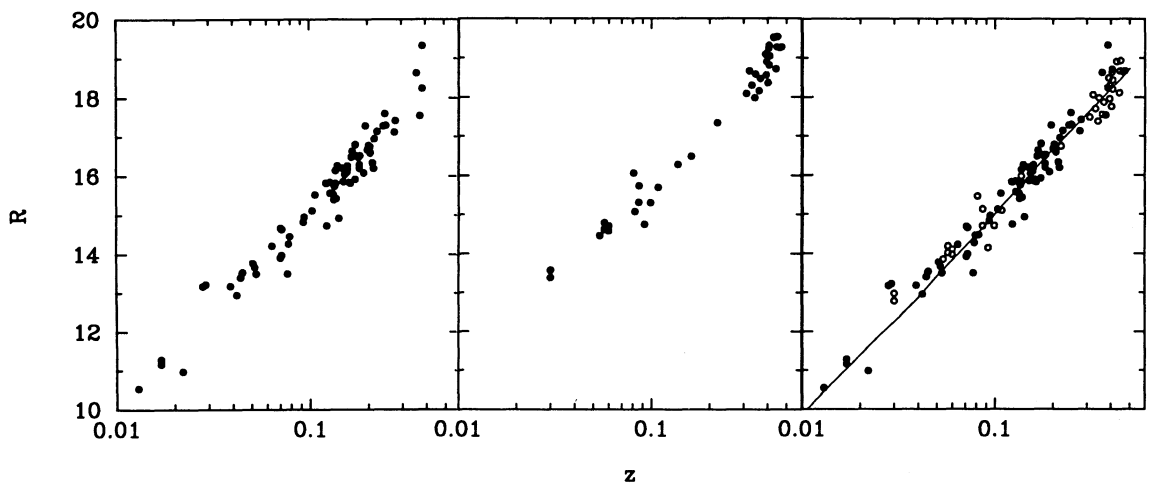

FIG. 6*a* FIG. 6*b* FIG. 6*c*

FIG. 6.—R band m-z relation for (*a*) brightest cluster members and (*b*) FR II radio galaxies. In (*c*) the FR II relation has been shifted by $\Delta R = -0.60$ and a smooth curve put through the data points.

and,

$$M_V = M_V^{\rm BCM} + m_{\rm gal} - m_{\rm E}(z, M_V^{\rm BCM}) + \frac{\partial M}{\partial C}\,[C_{\rm gal} - C_{\rm E}(z, M_V^{\rm BCM})] \quad (3)$$

Two of the sources in Table 1 with questionable photometry, PKS 1214+038 and PKS 1215+039, are both members of one cluster, which is rich enough to have a well-defined early-type galaxy sequence. We have used the location of this sequence, compared to that predicted by the above procedure, to correct the photometry in this field. However, because these objects represent a biased subset of all the sources with questionable photometry, these data are not included in the later analysis except when explicitly indicated.

3.2. *Tests*

The procedure outlined above allows one to map the observed color–apparent magnitude plane into the rest frame $B-V$ versus M_V plane. That this procedure works well at both low and high redshifts may be demonstrated by several tests. We construct the luminosity function of galaxies within the 500 kpc sample radius of all low-redshift and all high-redshift radio sources, correcting for field contamination using the offset frames. Since the regions were selected to be centered on a radio galaxy, always a bright elliptical-like object, inclusion of the radio galaxy would bias the luminosity function, and we therefore exclude it. If the galaxy luminosity function represents a probability distribution function, of which each galaxy is an independent sample, the remaining cluster members should provide an unbiased estimate of the group galaxy luminosity function.

Figure 7 compares the integrated luminosity functions of the low-redshift sample derived from the isophotal and aperture magnitudes. The two are virtually identical except for very luminous galaxies, whose extended envelopes are not encompassed by the apertures which we use. Figure 8 compares the integrated aperture magnitude luminosity functions of the low- and high-redshift samples. The agreement is excellent, suggesting that we have properly normalized both the low- and the high-redshift magnitude scales. That, in turn, suggests that whatever luminosity evolution occurred in the general galaxy population after the epoch observed at $z \approx 0.4$ was very similar to that which occurred in the brightest cluster members and strong radio galaxies which we have used to set the photometric zero point. Finally, in Figure 9 we compare the differential luminosity function of the combined low and high-redshift samples with a Schechter function of parameters $M_V^* = -21.9$, $\alpha = -1.25$. These parameters are a reasonable average, con-

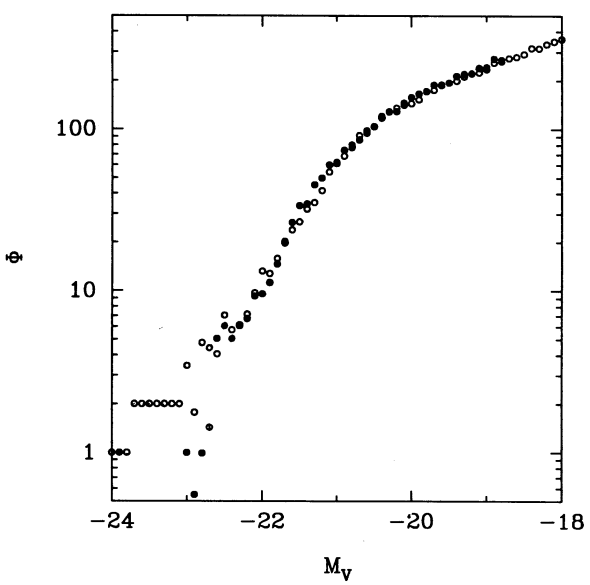

FIG. 7.—Integrated luminosity function of the low-redshift sample. *Filled circles:* aperture magnitudes; *open circles:* isophotal magnitudes.

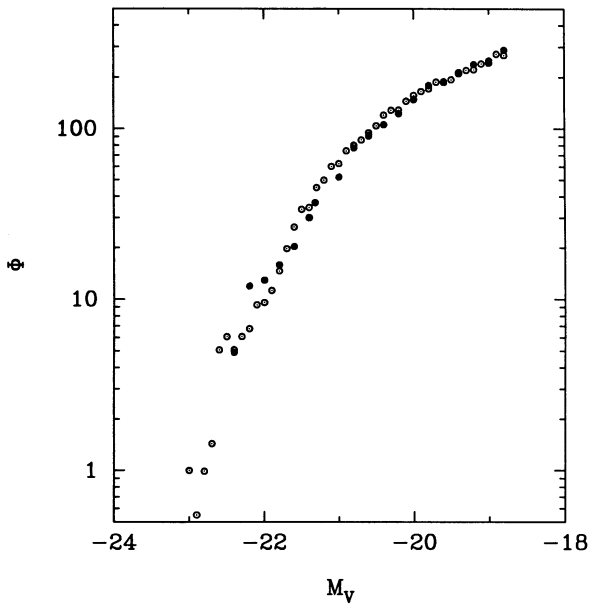

FIG. 8.—Integrated aperture luminosity functions. *Filled circles:* high-redshift sample; *open circles:* low redshift sample.

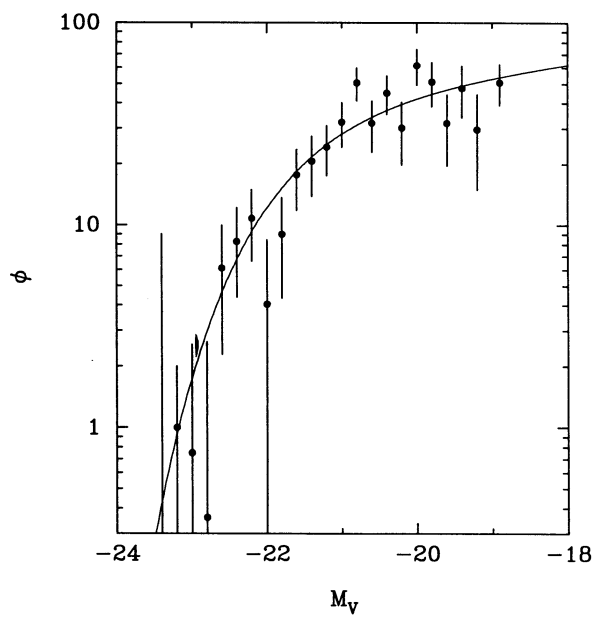

FIG. 9.—*Filled circles:* differential luminosity function of the combined low- and high-redshift samples. *Smooth curve:* Schechter function with parameters $\alpha = -1.25$, $M_V^* = -21.9$.

verted to the V band, of the various determinations of the field and cluster galaxy luminosity functions reported in Efstathiou, Ellis, & Peterson (1988), Schechter (1976), and Dressler (1978). This function fits the data quite well except at the very bright end, where the data fall below the function, probably because of the systematic departure of isophotal from aperture magnitudes which was seen in Figure 7.

We can test our colors using the analysis of the co-added, field-subtracted data to be presented later. We expect (see Butcher & Oemler 1979, B&O) the distribution of $\Delta(B-V)_0$ for normal galaxy populations to have a sharp peak at a value of 0.0. The co-added distributions of $\Delta(B-V)_0$ of the low and high-redshift samples are presented in Figures 17 and 18. The low-redshift distribution does peak at $\Delta(B-V)_0 = 0.00 \pm 0.02$, confirming the correctness of its color zero point. The high-redshift distribution in Figure 18 seems to be offset from 0.0 by about 0.025 mag. We shall take this offset into account in the later analysis. Finally, in Figure 10 we present the $\Delta(B-V)_0$ versus M_V distribution for the cluster surrounding the high-redshift source 4C 29.44, which is by far the richest group in our sample. That the data points scatter about $\Delta(B-V)_0 = 0.$ by an amount consistent with the error bars suggests that the measured colors in this (completely red) cluster have correct zero points and error estimates.

4. RESULTS

Our dataset allows us to address the present properties and past evolution of three characteristics of the population of galaxies associated with radio galaxies: (1) the galaxy luminosity function, (2) the richness of the groups in which they occur, and (3) the stellar populations of the galaxies. We have briefly examined the luminosity functions of the low- and high-redshift populations and found them to be indistinguishable from those of nearby field galaxies. In the following sections, we address the other two properties.

4.1. *Group Richness*

In the rest frame $\Delta(B-V)_0$ versus M_V plane, our sample consists of all objects classified as galaxies with $M_V \leq -19.0$ and within 0.5 Mpc radius of the radio galaxy. The latter specification depends, of course, on q_0, but not with great sensitivity. We assume a value $q_0 = 0.0$; if we had used $q_0 = 0.5$, the angular distance corresponding to 0.5 Mpc would increase by 10% at $z = 0.4$. We find empirically that, for radii near 0.5 Mpc, the richnesses of our groups vary with radius as

$$N_{\rm gal} \propto r^{0.8} . \quad (4)$$

Thus, a choice of $q_0 = 0.5$ would increase our high-redshift group richnesses by only 8%. The deduced galaxy population of each group was corrected for background contamination using the nearby offset region. A few radio galaxies have no corresponding offset region observations. Their populations were calculated using the mean of three or four offset regions near the closest radio galaxies surveyed in the same part of the sky. Some of the lowest redshift galaxies do not have photometry covering the full 0.5 Mpc radius area. We corrected the group richnesses of these sources using equation (4), and shall correct the group color distributions in a manner to be described later. Those requiring large (a factor of 1.8 or more) richness corrections are noted in Table 1. A few of the high-redshift galaxy fields were not complete to $M_V = -19.0$. These have been corrected using a Schechter luminosity function with parameters $M_V^* = -21.9$ and $\alpha = -1.25$. Those with corrections larger than 20% are noted in Table 2. We denote the richness within the limits defined above as $N_{0.5}^{-19}$ and present its value for each group in column (6) of Tables 1 and 2; this number includes the radio galaxy. Errors were calculated from the Poisson statistics of the group and background counts and are presented in column (7) of the same tables. In Table 4 we summarize mean and median values of $N_{0.5}^{-19}$ for various subsets of the data. Because the distribution of this quantity is very non-Gaussian, errors were calculated by the bootstrap method (Barrow, Bhvasar, & Sonoda 1984) and are presented in Table 4 as 67% confidence limits.

Previous studies of clustering around radio galaxies have been published by Prestage & Peacock (1988, hereafter P&P), Yates, Miller, & Peacock (1989), and Hill & Lilly (1991, hereafter H&L). The latter paper, in particular, contains a large body of high-quality data on high-redshift sources, based on CCD photometry, and analyzed in a manner similar to ours. In order to increase the size of our dataset, we shall incorporate their data with our own. Their data consists of photometry of 42 radio galaxies with $0.37 < z < 0.55$, plus three radio galaxies with photometrically estimated redshifts of about 0.64. Like ourselves, H&L count galaxies within 0.5 Mpc of the radio galaxy. Unlike our procedure, they do not separate stars

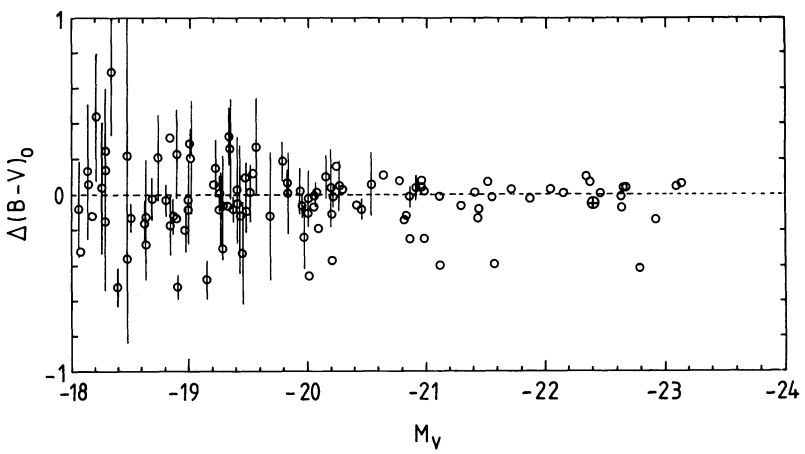

FIG. 10.—Rest frame color-magnitude diagram for the high-redshift cluster surrounding 4C 29.44.

TABLE 4

SAMMARY OF SAMPLE RICHNESSES

SAMPLES					$N_{0.5}^{-19}$	
Number	Redshift	Table	SUBSET	N_{group}	Median	Mean
1	Low	1	All	65	$4.5^{+2.5}_{-0.6}$	7.2 ± 1.0
2			FR I	15	$10.0^{+4.8}_{-2.7}$	12.4 ± 2.6
3			FR II	28	$4.1^{+1.3}_{-1.3}$	6.0 ± 1.3
4			$\log P_{408} < 26.7$	37	$4.5^{+2.6}_{-0.6}$	7.2 ± 1.2
5			$\log P_{408} \geq 27.2$	28	$5.2^{+2.5}_{-2.6}$	7.1 ± 1.8
6	High	2	All	33	$8.4^{+2.4}_{-2.4}$	10.9 ± 2.5
7	High	5	All	34	$8.0^{+2.0}_{-1.1}$	10.3 ± 1.6
8	High	2, 5	All	58	$8.0^{+1.9}_{-0.9}$	10.1 ± 1.6
9			FR II	33	$9.1^{+2.1}_{-1.2}$	12.2 ± 2.4
10			NOT FR II	25	$6.2^{+2.6}_{-1.7}$	8.4 ± 2.0
11			$\log P_{408} < 27.2$	30	$8.0^{+2.6}_{-1.4}$	9.3 ± 1.6
12			$\log P_{408} \geq 27.2$	28	$8.6^{+1.6}_{-2.0}$	12.0 ± 2.9

TABLE 5

HILL AND LILLY SAMPLE

IAU	Other	z	$\log P_{408}$	FR	$N_{0.5}^{-19}$
0822+34A.....	B2	0.406	27.18	II	1 ± 8
0824+29.....	3C 200	0.458	27.89	II	1 ± 6
0832+45.....	55W010	0.452	26.00	C	9 ± 11
0833+45.....	55W016	0.375	25.11	...	0 ± 7
0833+45.....	55W023	0.360	24.90	...	1 ± 7
0835+37.....	B2	0.396	26.68	C	23 ± 8
0838+44.....	55W097	0.365	24.20	...	14 ± 7
0841+44.....	...	0.425	24.00	I?	-11 ± 8
0842+45.....	55W150	0.465	24.40	...	6 ± 11
0843+44.....	55W161	0.402	24.48	...	4 ± 9
0847+37.....	B2	0.407	27.03	II	22 ± 10
1030+58.....	3C 244.1	0.428	28.26	II	25 ± 12
1104+36.....	B2	0.393	27.18	II	8 ± 10
1201+39.....	B2	0.445	27.07	II	9 ± 8
1203+64.....	3C 268.3	0.371	27.85	II	8 ± 6
1232+21.....	3C 274.1	0.422	27.98	II	10 ± 7
1239−04.....	3C 275	0.480	28.18	II	1 ± 1
1245+34.....	B2	0.420	27.00	II	20 ± 7
1255+35.....	5C 12.71	0.436	25.75	I	8 ± 7
1256+37.....	5C 12.91	0.464	25.96	II	21 ± 10
1259+37.....	5C 12.168	0.424	25.77	I	4 ± 6
1301+34.....	5C 12.217	0.428	26.08	II	7 ± 8
1301+38A.....	B2	0.470	27.32	II	1 ± 7
1302+36.....	5C 12.241	0.487	26.89	II	8 ± 8
1303+35.....	5C 12.264	0.373	26.00	C	10 ± 8
1307+34.....	5C 12.304	0.460	26.38	C	23 ± 8
1409+52.....	3C 295	0.461	28.72	II	29 ± 18
1419+41.....	3C 299	0.367	27.78	C	4 ± 6
1452−04.....	3C 306.1	0.441	27.69	II	5 ± 10
1508+08.....	3C 313	0.461	28.15	II	28 ± 14
1626+27.....	3C 341	0.448	27.84	II	7 ± 10
1715+49.....	53W032	0.370	25.30	...	14 ± 9
1715+50.....	53W039	0.402	24.90	...	16 ± 9
1719+49.....	53W076	0.390	24.60	C	14 ± 9

from galaxies. More importantly, they count over a magnitude interval from the radio galaxy to 3.0 mag fainter, rather than over a fixed range of absolute magnitude.

We have nine radio galaxies in common with H&L. If we analyze our data in exactly the same manner as H&L, including stars and counting to $M_{RG} + 3.0$, we find, for these nine sources, a ratio of H&L's counts to ours of 1.46 ± 0.44, suggesting a possible systematic difference. That this difference is not significant can be demonstrated with a larger sample, which we construct by converting to our system the data on all H&L radio sources with $z < 0.50$. Using a Schechter function with parameters $\alpha = -1.25$, $M_V^* = -21.9$, we correct the H&L counts to a limiting magnitude of -19.0. The resulting values of $N_{0.5}^{-19}$ for these 34 sources are presented in Table 5, in a format similar to Tables 1 and 2. We have converted the radio powers at 2 GHz, reported in their Table 1, to powers at 408 MHz using published spectral indices. If none was available, we have assumed a radio spectral index $\alpha_R = -0.75$ (where $f_\nu \propto \nu^{\alpha R}$). We have accepted their classifications of FR type, except for those weak sources which they assigned class I?, based on an assumed trend of FR type with radio power. We prefer to type these as unknown class. The distributions of $N_{0.5}^{-19}$ for this subset of the H&L sample and for our own high-redshift sample from Table 2 are presented in Figure 11. The distribution of H&L richnesses is, within the errors, identical to that of our groups (Table 4, samples 6 and 7).

The group richnesses of the low-redshift sample, from Table 1, and of the combined high-redshift sample, from Tables 2 and 5, are plotted versus radio power, in Figures 12*a* and 12*b*, respectively. There appears to be no trend of richness with radio power within either sample (see Table 4, samples 4 vs. 5 and 11 vs. 12). The slightly higher mean in sample 12 is entirely attributable to the one unusually rich source 4C 29.44. The high-redshift groups in Figure 12*b* appear, however, to be somewhat richer, in the mean, than the low-redshift groups in Figure 12*a*, suggesting that group richness has decreased with epoch, as has been claimed by Yates et al., and by H&L. H&L find a mean difference of a factor of 2.5 between the richness of their sample, and that of a corresponding low-redshift sample constructed from the data of Prestage & Peacock. Their difference is in the same sense but much larger than we find: Table 4 shows that the mean of samples 1 and 8 differ by a factor of 1.36 ± 0.25. A Mann-Whitney U-test rejects the hypothesis that the two samples are identical at only an 88% confidence level. H&L found a difference among their FR II sources which was even larger than the factor of 2.5 derived from their entire sample. If we examine that subset (samples 3 and 9 of Table 4), we also find a stronger effect. The means of the two samples

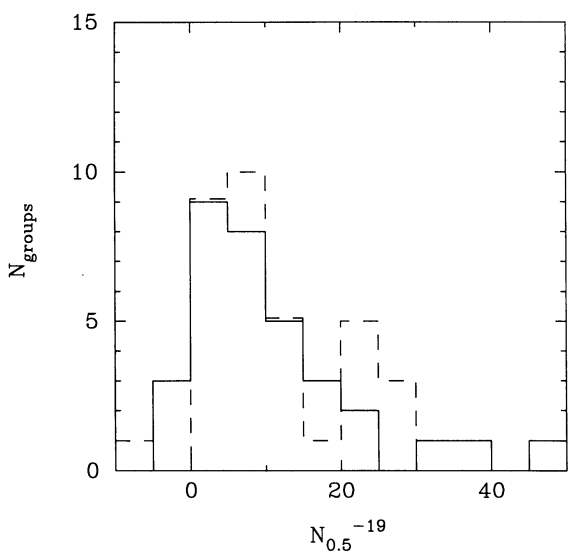

FIG. 11.—Distribution of group richness, $N_{0.5}^{-19}$, in our high-redshift sample from Table 2 (*solid line*) and the Hill & Lilly sample (*dashed line*).

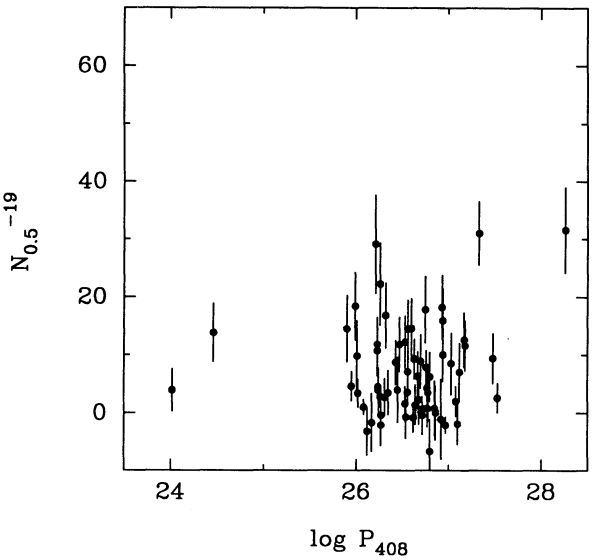

FIG. 12*a*

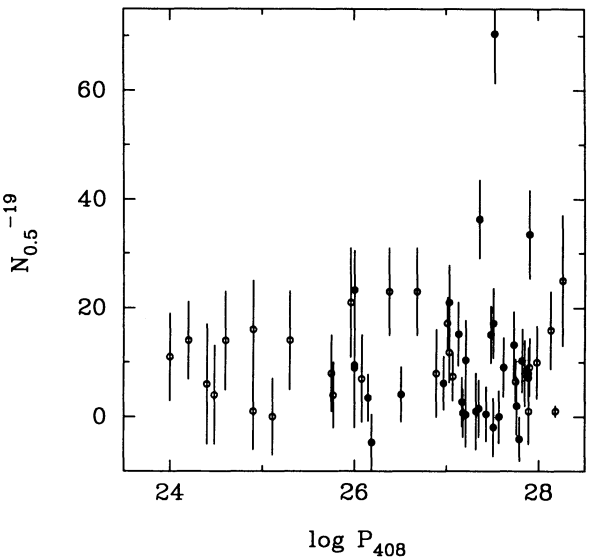

FIG. 12*b*

FIG. 12.—Group richness, $N_{0.5}^{-19}$, vs. radio power: (*a*) Low-redshift sample from Table 1. (*b*) High-redshift samples from Table 2 (*filled circles*) and Table 5 (*open circles*).

now differ by a factor of 1.84 ± 0.34, and the confidence level of the U test rises to 97%.

In summary, although we find qualitatively similar results to those of H&L, our data suggest rather less evolution than they claimed. We believe that our result is more reliable for two reasons: because the combined high-redshift sample is larger, and more importantly, because our comparison is based on more homogeneous data. H&L have no low-redshift data of their own. Instead, they have used the P&P values of the spatial correlation amplitude, B_{gg}, converted to their system of $N_{0.5}$ by an indirect process. The P&P B_{gg} values are fits to a $r^{-1.8}$ correlation function of the numbers of galaxies within 1 Mpc of the radio source, obtained primarily from the Shane & Wirtanen (1967) galaxy counts. These counts will inevitably be much less reliable than those obtained by CCD photometry since they are based on the visual inspection of photographic plates. Also, even if accurately limited by apparent magnitude, this limit corresponds to widely varying absolute magnitudes over the redshift range of the radio galaxies studied, necessitating large corrections.

We conclude, then that there has been, at most, mild evolution in the strength of clustering around FR II sources since the epoch observed at $z = 0.45$. Apparently this evolution is confined to FR II sources. We do not have many confirmed FR I sources at high redshift, but if we compare the high-redshift sources that are *not* confirmed FR II's, with the low-redshift FR I sources (sample 10 vs. 2) we find a weak trend in the opposite direction: the mean $N_{0.5}^{-19}$ of these samples is higher at low redshift. This suggests that the observed evolution is in the FR types of sources in rich environments, rather than in the richness of the environments themselves. We shall return to this subject in a subsequent paper.

It is also of interest to know how the properties of the radio groups compare with those of groups in general. The best available catalog of optically selected groups is that of Geller & Huchra (1983). This catalog was assembled by searching for enhancements in the space density of galaxies in the CfA redshift survey. For each group, Geller & Huchra report the total number of group members brighter than $B_{\rm lim} = 14.5$, within a density contour $\rho = 20\,\langle\rho\rangle$, where $\langle\rho\rangle$ is the mean density of galaxies within their sample volume. We convert this number to $N_{0.5}^{-19}$, the number of galaxies with projected distances from the group center less than 0.5 Mpc, and with $M_V \leq -19.0$ by the following procedure. Assuming $\langle B-V\rangle = 0.75$, and assuming a galaxy luminosity function of the Schechter form with parameters $M_V^* = -21.9$, $\alpha = -1.25$, we convert the richness of each group brighter than $B_{\rm lim} = 14.5$, $N^{14.5}$ to the richness brighter than $M_V = -19.0$, which we denote N^{-19}. To convert from $N_{\rho 20}$, the number interior to $r = 20\,\langle\rho\rangle$ to $N_{0.5}$, the number within 0.5 Mpc, we use the density profiles of clusters described in West, Dekel, & Oemler (1987). Assuming a mean luminosity density for the universe of $1.17 \times 10^8\ L_\odot$ Mpc^{-3} (Kirshner et al. 1983), the cluster luminosities reported in West, Oemler, & Dekel (1989) allow us to express these profiles in units of $\rho(r)/\langle\rho\rangle$, and locate the $\rho = 20\,\langle\rho\rangle$ contour. From this we find

$$N_{0.5} = 1.9(N_{\rho 20})^{0.6}\ . \tag{5}$$

The correction from limits of $B = 14.5$ to $M_V = -19.0$ requires, in general, an extrapolation, which introduces large statistical uncertainties if either $N_{\rho 20}^{14.5}$ is small or $N^{-19}/N^{14.5}$ is large. To minimize these uncertainties, we restrict our sample to those groups with $N_{\rho 20}^{14.5} \geq 4$ and $500 < cz \leq 5000$ km s^{-1}. Then, to calculate the space density of groups as a function of $N_{0.5}^{-19}$, we must take account of the distance selection effects. This is a straightforward task. For each value of $N_{0.5}^{-19} = f(N_{\rho 20}^{-19})$, there is a maximum distance, and equivalent maximum recessional velocity, $v_{\rm max}$, at which there will be at least four galaxies in the group brighter than $B = 14.5$, and the volume from which groups of this $N_{0.5}^{-19}$ will be drawn is that between 500 km s^{-1} and $v_{\rm max}$. The space density of these groups is, then, just the number in our sample divided by this volume.

The results of this analysis are given in Figure 13, in which the cumulative distribution of CfA group richnesses is presented as the thin solid line. Because the differences between the

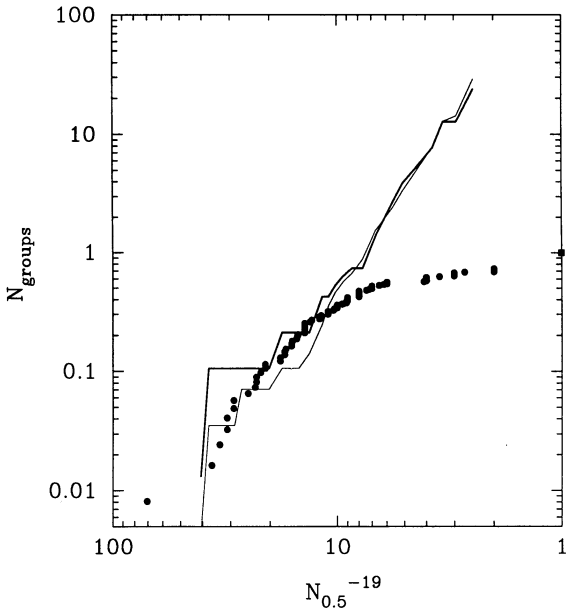

FIG. 13.—Cumulative distribution functions of group richness. *Thin solid line:* all CfA groups; *thick solid line:* CfA groups with brightest elliptical members; *points:* sum of all low- and high-redshift radio groups from Tables 1, 2, and 5.

total low- and high-redshift radio source group populations are minimal, we combine all the data from Tables 1, 2, and 5 and present the cumulative richness distribution of these 122 groups in Figure 13. as filled circles. This line has been shifted vertically to align it with the CfA distribution. These data are not inconsistent with radio galaxies occurring with equal frequency in groups of every richness above $N_{0.5}^{-19} = 12$, but it is clear that their frequency in poorer groups is much lower. However, a simulation of the process of group selection (Moore, Frenk, & White 1992) indicates that group-finding algorithms similar to that used by Geller & Huchra will inevitably find large numbers of spurious poor groups. Such contamination of the CfA group catalog may be responsible for all or part of the difference in the richness distributions of the radio and optically selected samples. Nevertheless, whether this interpretation of the difference in the two richness distributions is correct or not, it is a fact that many radio galaxies are in small groups.

It is arguable whether one should compare the groups around radio galaxies to groups in general. Since powerful radio galaxies are generally elliptical and the brightest members of their groups (Lilly & Prestage 1987), one might wish to compare radio groups with that subset of optically selected groups whose brightest member is an elliptical. The well-known dependence of galaxy properties on environment, which we shall call the morphology-environment relation, would suggest that this subset would contain fewer poor groups and might more closely resemble the radio-selected sample. We have, therefore repeated the above analysis with that subset of the CfA groups which satisfy this criterion. The results are presented in Figure 13 as a heavy solid line, which has been shifted vertically to align it with the other curves. In fact, the distribution of richnesses of these groups differs little from that of all optical groups, although the richest groups are somewhat better respresented among this sample. We shall consider the implications of these points further in a subsequent paper.

Using the same West et al. cluster profiles, we may convert our richnesses to the richness scale of the Abell catalog of clusters (Abell 1958). We derive that

$$N_{\rm Abell} = 0.35(N_{0.5}^{-19})^{1.4} . \quad (6)$$

The reason for the nonlinearity of equations (5) and (6) is simple: richer groups are larger, and a smaller fraction of their population is contained within a projected radius of 0.5 Mpc. With this calibration, we find that 96% of the groups are poorer than richness class 0. There are four of 123 which are of richness class 0, none of richness class 1, and one exceptional cluster, that around 4C 29.44, is of richness class 2.

4.2. *The Colors of Group Members*

We shall describe the galaxy populations in the radio groups by the distribution of the quantity $\Delta(B-V)_0$, which we have defined to be the rest frame $B-$V color of a galaxy relative to the color of the early-type galaxies of the same absolute magnitude. Following B&O, we define f_B be the fraction of galaxies with $\Delta(B-V)_0 \leq -0.20$. Because the contrast of these groups above the background is very low, the accuracy of these determinations can be improved by restricting analysis to that range of $\Delta(B-V)_0$ which is occupied by galaxies. Analysis of the distribution of $B-V$ colors of galaxies in the Second Reference Catalog of Bright Galaxies (de Vaucouleurs, de Vaucouleurs, & Corwin 1976, hereafter RC2), and of the distribution of $\Delta(B-V)_0$ values in the low- and high-redshift samples, presented in Figures 17 and 18, show that almost all galaxies occupy the range $-0.6 \leq \Delta(B-V)_0 \leq 0.25$. Values outside this range are undoubtedly due to stars, QSOs, and foreground and backgound galaxies. We shall, therefore, calculate f_B using only objects within this range of $\Delta(B-V)_0$. Values of f_B, for those groups sufficiently rich to permit its calculation, are presented in the eighth columns of Tables 1 and 2.

In those cases (all noted in Table 1) where photometry did not cover the entire inner 0.5 Mpc of the group, a correction to f_B is needed, since blue fractions tend to rise with increasing distance from the group center. We have examined the cluster photometry from B&O (see B&O, Fig. 5), as well as the group data reported in this paper, and find very similar trends of f_B with radius, independent of richness or absolute values of f_B. In the range of radii near 0.5 Mpc, we find that the variation of f_B with limiting radius $r_{\rm lim}$, can be approximated by

$$\Delta f_B = 0.24 \log (r_{\rm lim}/0.5 \text{ Mpc}) . \quad (7)$$

Typical adjustments to f_B are only a few hundredths. Where needed, we apply these corrections to the individual richer groups in Table 1. We also apply them to the average values for collections of radio groups to be discussed later, using mean corrections weighted by $N_{0.5}^{-19}$. The errors listed in the ninth columns of the tables are derived from count statistics. To this we have added in quadrature $0.5\Delta f_B$ as a generous estimate of the uncertainty in that correction.

Figures 14 and 15 present the distribution of f_B with radio power of groups in the low- and high-redshift samples. Individual groups are indicated by open circles. To include those groups to poor for individual determinations of f_B, the color distributions of all groups in ranges of radio power have been combined, and f_B calculated from the summed distributions. These mean values are indicated by filled circles and are tabu-

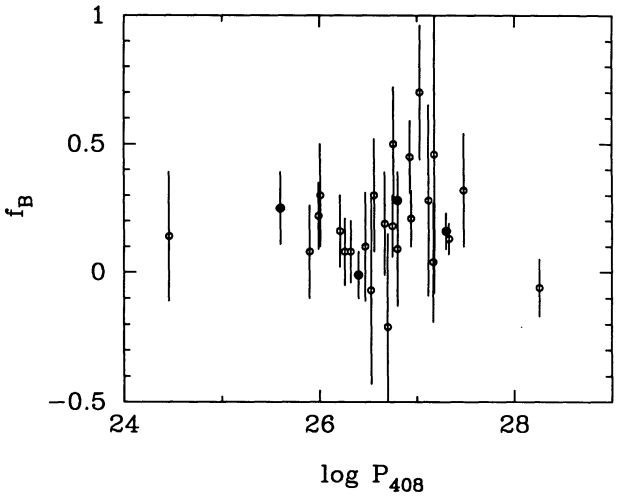

FIG. 14.—Blue fraction vs. radio power of low-redshift sample. *Open circles:* individual groups; *filled circles:* average of all groups in interval of radio power.

lated in Table 6. PKS 1214+038, and PKS 1215+039 are included in Figure 14 and subsequent plots as individual clusters, but their photometry has not been included in forming average values. None of these distributions shows a significant trend of galaxy population with radio power. Thus, at least within the range of power $10^{26} < P_{408} < 10^{28}$ W Hz^{-1}, neither the number nor the type of galaxies surrounding a radio galaxy are sensitive to the radio power. Since radio power was the sole selection criterion of our samples, we are confident that our technique has produced unbiased samples, which may be used to study the evolution of group galaxies in general. The lack of dependence on radio power also reassures us that the mistaken inclusion of 5C 3.100 and 5C 3.175 has not compromised our results.

As a further test of how our radio groups are representative, we compare values of f_B for the radio groups and for optically selected groups and clusters. We calculate f_B for the CfA groups from the morphological types reported in Geller & Huchra (1983), assuming that group galaxies have the same

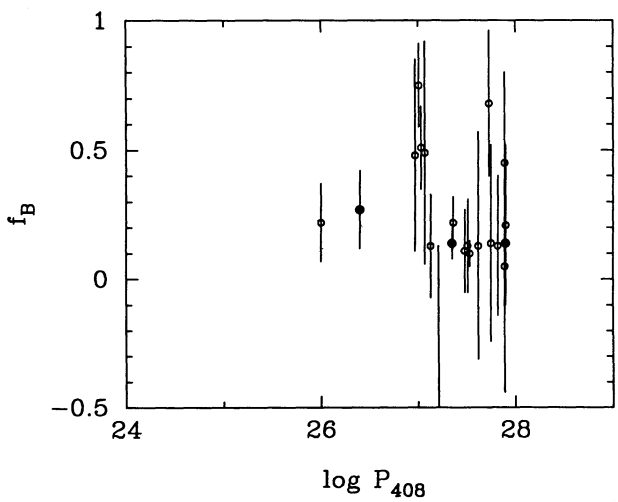

FIG. 15.—Blue fraction vs. radio power of high-redshift sample. *Open circles:* individual groups; *filled circles:* average of all groups in interval of radio power.

TABLE 6

SUMMARY OF SAMPLE f_B VALUES

Sample				
Redshift	Selection	Subset	N_{groups}	f_B
Low	Radio	All	65	0.19 ± 0.05
		$\log P_{408} < 26.2$	8	0.25 ± 0.14
		$26.2 \le \log P_{408} < 26.6$	11	-0.01 ± 0.09
		$26.6 \le \log P_{408} < 27.0$	16	0.28 ± 0.11
		$\log P_{408} \ge 27.0$	9	0.16 ± 0.07
		$N_{0.5}^{-19} < 8$	29	0.16 ± 0.23
		$8 \le N_{0.5}^{-19} < 13$	7	0.27 ± 0.09
		$13 \le N_{0.5}^{-19} < 20$	7	0.26 ± 0.06
	Optical (any BCM)	$N_{0.5}^{-19} < 7$	42	0.51 ± 0.05
		$7 \le N_{0.5}^{-19} < 12$	30	0.37 ± 0.04
		$12 \le N_{0.5}^{-19} < 20$	5	0.34 ± 0.14
	Optical (E BCM)	$N_{0.5}^{-19} < 7$	15	0.38 ± 0.13
		$7 \le N_{0.5}^{-19} < 12$	8	0.26 ± 0.15
		$12 \le N_{0.5}^{-19} < 20$	3	0.30 ± 0.16
High	Radio	All	33	0.15 ± 0.05
		$\log P_{408} < 27.0$	4	0.22 ± 0.15
		$27.0 \le \log P_{408} < 27.7$	14	0.14 ± 0.06
		$\log P_{408} \ge 27.7$	15	0.14 ± 0.10
		$N_{0.5}^{-19} < 8$	16	-0.03 ± 0.27
		$8 \le N_{0.5}^{-19} < 13$	7	0.02 ± 0.13
		$13 \le N_{0.5}^{-19} < 20$	5	0.29 ± 0.09

distribution of $B-V$ colors as do galaxies of the same morphological type with colors reported in the RC2. This assumption must be justified: there is evidence (Oemler 1992) that spiral galaxies in rich clusters are redder than those of the same type in the field. To do this we have compared the mean color of CfA group members of each morphological type in the RC2, with that of all catalog galaxies of that type. No differences were found. Average values for three intervals of $N_{0.5}^{-19}$ are presented in Table 6 and are shown by open squares in Figure 16. We do the same for that subset of CfA groups whose brightest member is an elliptical. These values are also presented in Table 6 and are shown in Figure 16 as open diamonds.

To extend our study to include rich clusters, we take data from B&O, correcting both f_B values and richnesses to those appropriate to a 0.5 Mpc radius. We use all rich clusters, including those of irregular structure which are significantly richer in spiral galaxies than is the typical cluster, since we have no corresponding structural information on the groups that would allow us to so classify them. From the same paper we take a value $f_B = 0.41 \pm 0.10$ for the field. These data are presented in Table 6 and shown in Figure 16 as open circles. Finally, the radio groups are shown in Figure 16 as filled circles. Groups with $N_{0.5}^{-19} > 20$ are plotted individually. Poorer groups are combined into intervals of richness; for the radio groups these are $-\infty < N_{0.5}^{-19} < 8$, $8 \le N_{0.5}^{-19} < 13$, and $13 \le N_{0.5}^{-19} < 20$.

This plot shows that the blue galaxy content of low-redshift groups is a strongly decreasing function of their richness. The smooth curve is one possible eye fit to the data. It is by no means unique: a more steplike function would be equally consistent. The qualitative trend is, however unambiguous: poor groups have galaxy contents (as measured by their colors) like that of the field, while rich clusters are devoid of blue galaxies. Optical groups with elliptical brightest group members are slightly redder than other groups and appear to have galaxy

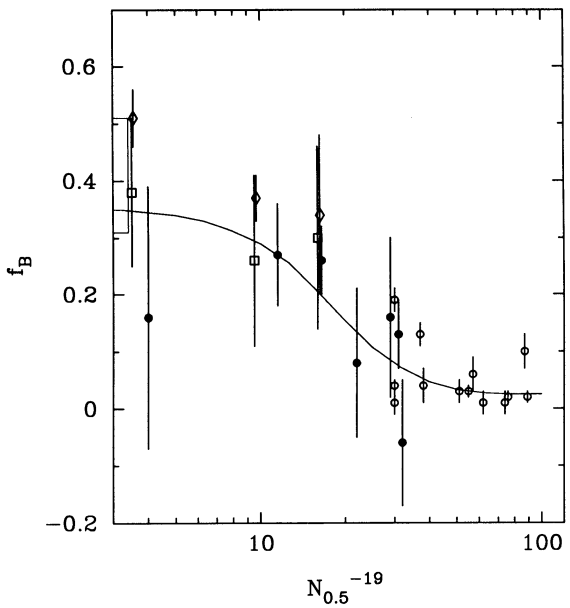

FIG. 16.—Blue fraction vs. group richness of the low-redshift sample. *Filled circles:* radio groups; *open squares:* all CfA groups; *open diamonds:* CfA groups with brightest elliptical members; *open circles:* rich clusters; *rectangular area:* field galaxies; *solid line:* eye fit to trend.

contents very similar to those of radio groups of the same richness. Combined with the similarity in luminosity functions demonstrated in Figure 9, these results demonstrate that the galaxies in groups surrounding radio galaxies are not at all unusual, and can be taken to be representative of the populations of groups of galaxies in general.

4.3. *Evolution in the Morphology-Density Relation*

The dependence of galaxy color on group richness is, of course, no surprise; it is a reflection of the general relationships between color and morphology, and between morphology and environment, which have been shown to operate in galaxy associations of a wide range of richness. Whether this relation is due to a physical dependence on local density, global cluster properties, or some other variable is of little importance to us. As long as the underlying physical relations are reflected in a dependence of galaxy color on group richness, we can use the latter as an indicator of the existence of a morphology-environment relation.

We are now in a position to compare the galaxy contents of high-redshift groups with those at low redshift. Summing all low-redshift groups and all high-redshift groups, we obtain the distributions of $\Delta(B-V)_0$ presented in Figures 17 and 18, and mean values of f_B presented in Table 6. The import of these distributions is clear: contrary to the situation in rich clusters, galaxies in small groups are *not* significantly bluer at high redshift. Between $z = 0.00$ and $z = 0.40$, we find a bluing of only $\Delta f_B = -0.05 \pm 0.07$, whereas in rich clusters B&O found $\Delta f_B = +0.15$. The difference in these two trends two trends is significant at the 99.5% level. Thus, the evolution seen in rich clusters is not typical of that occurring in all galaxy populations; galaxy evolution is, evidently, dependent on environment.

The nature of that dependence is revealed by comparing Figure 16 with the corresponding high-redshift data, which is presented in Figure 19 and summarized in Table 6. The optical

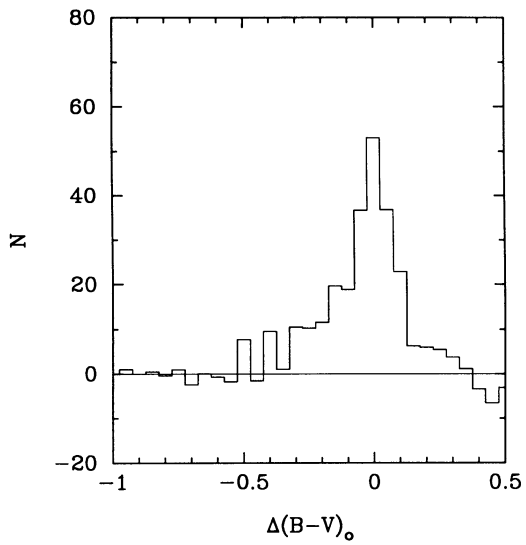

FIG. 17.—Distribution of $\Delta(B-V)_0$ for the members of all groups in the low-redshift sample.

data come from the observations of rich clusters presented in B&O, adjusted to the limits of $M_V = -19.0$ and $R_{\rm lim} = 0.5$ Mpc, with data from one additional cluster recently observed by Molinari, Buzzoni, & Chincarini (1990). The radio groups are subdivided into the same intervals of richness as at low redshift. The eye fit to the low-redshift data in Figure 16 has been translated to this plot. It is clearly not a good representation of the high-redshift data, nor would it be even if shifted to higher values of f_B. While the galaxy content of rich clusters has evolved substantially since the epoch observed at $z = 0.4$, that of poor groups has not evolved at all. As a consequence of this differential evolution, there is virtually no color-environment relation at $z = 0.4$. We have no direct structural information on these high-redshift galaxies and can, therefore make no blanket statements about the morphology-environment relation at earlier epochs. However, since the Hubble type of a galaxy is very dependent on the amount of

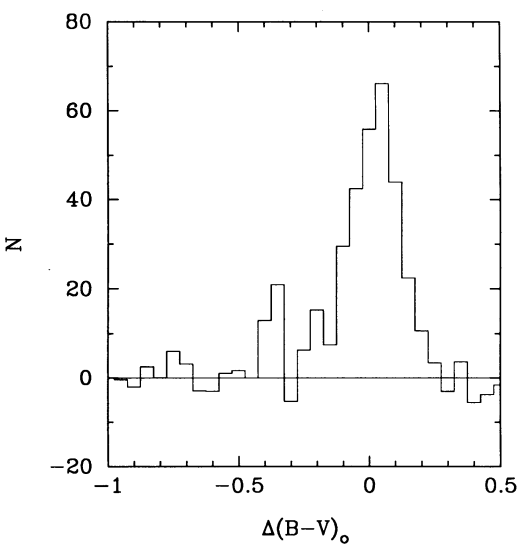

FIG. 18.—Distribution of $\Delta(B-V)_0$ for the members of all groups in the high-redshift sample.

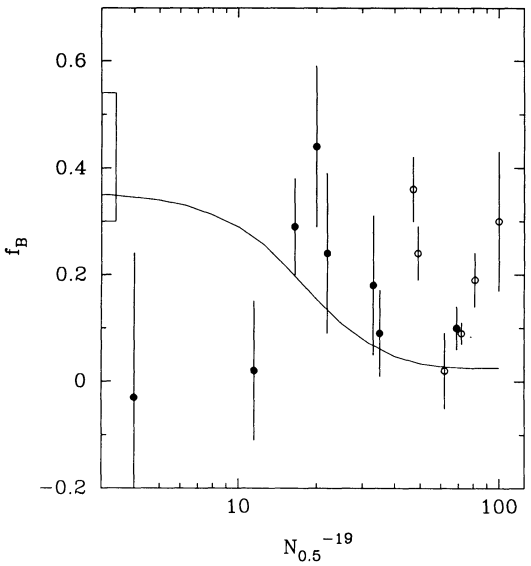

FIG. 19.—Blue fraction vs. group richness of the high-redshift sample. *Filled circles:* radio groups; *open circles:* rich clusters; *rectangular area:* field galaxies; *solid line:* eye fit to low-redshift data from Fig. 17.

star formation, and the latter is reflected in its color, the lack of a color-environment relation at $z = 0.4$ virtually requires that the morphology-environment relation then be different that it is today.

Given the different evolutionary behaviour found in groups and rich clusters, the question of how this trend extrapolates to the general field arises. It is now well established that there exists a significant population of faint blue galaxies in excess of the "no-evolution" prediction (cf. Kron, Sprinrad, & King 1977; Peterson et al. 1979; Tyson 1988). Early explanations (cf. Bruzual & Kron 1980, Koo 1981) suggested that bluing of the field population with lookback time is responsible, arising from an increase in the bulk star formation rate. In fact, many early reviews drew attention to the similarity between this behavior and the rising blue fraction in the cores of rich clusters. If this were the case, any similarity between the field and rich clusters would be difficult to reconcile with the results for the groups.

However, deep redshift surveys (Broadhurst et al. 1988; Colless et al. 1990; Lilly, Cowie, & Gardner 1991) have revealed the field situation to be considerably more complex, and the precise explanation for the excess blue population is still a matter of much debate. It appears that some form of apparent *number* evolution is required, either via a hitherto undiscovered new population (Babul & Rees 1991) or via widespread merging associated with an increased star formation rate (Broadhurst, Ellis, & Glazebrook 1992). Ideally, it is desirable to quantify the amount of field evolution by the same measures we have applied to groups and clusters, but the extant data are very different. In the field surveys, the samples are apparent magnitude–limited and cover a range of redshifts with strong luminosity and color-dependent biases which must be carefully accounted for. For example, because the blue-shifted effective wavelength of the b_J band used for the surveys is in the ultraviolet at $z \simeq 0.4$, the magnitude limit corresponds to a V luminosity which is a steep function of color with bluer galaxies being strongly favored.

As an example of how this might be done, we apply our techniques to the AAT survey of Colless et al. where $b_J - r_F$ colors and redshifts are available for a near-complete sample with $21 < b_J < 22.5$. By making an additional correction for the variation of limiting magnitude with color, we reduce these data to a rest frame M_V versus $B - V$ plane. As in the analysis of H&L's data, we assume a Schechter luminosity function for all galaxies regardless of color, with $M_V^* = -21.9$, $\alpha = -1.25$. Restricting our analysis to Colless et al. galaxies with $0.3 < z < 0.5$, we find $f_B = 0.42 \pm 0.12$: a value similar to that for local field galaxies and for the radio groups in both redshift ranges (cf. Fig. 19).

While this result supports the conclusions derived from our groups, it is rather surprising when one considers that the faint blue excess population is calculated with respect to "no-evolution" predictions which carefully allow for precisely those biases addressed above with the AAT data. Thus, on one hand, the f_B analysis of the AAT survey requires little color evolution for a fixed luminosity range, yet the blue objects indicate a definite increase in the luminosity density of blue objects. It may be possible to understand the apparent contradiction by noting that only a small change of f_B within our error band is likely to have a more profound effect on the *counts* than on the color distribution, because of the luminosity change associated with any star formation change, particularly if the activity is sharply peaked in time. Additionally, if a new population is responsible for the bluing, either via extra merging subunits or a population of bursting dwarfs that decay beyond detection by the present epoch, it may be possible to reconcile an unchanging f_B for the underlying "quiescent" population with the group results. The apparent conflict is an important result which may throw valuable new light on the question of the origin of the faint blue field galaxies. However, because of this, we postpone a major discussion to a later paper.

5. DISCUSSION

The results presented in the previous section provide significant constraints on possible models for the evolution of galaxies. It is, for example, clear that the hypothesis, advanced by B&O, that the recent evolution of stellar populations in galaxies is an internally driven process, occurring in galaxies everywhere, is untenable. Such a model would predict evolution in small groups and the field to be at least as rapid as in rich clusters, and probably more rapid, since they have more gas-rich galaxies. One would then expect the trend of f_B with N to be higher and steeper at $z = 0.4$ than at $z = 0.0$.

The most straightforward conclusion which could be drawn from these findings is that the morphology-environment relation has evolved rapidly during the last third of the age of the universe. Galaxy populations were rather homogeneous at the epoch observed at $z = 0.4$ and have differentiated themselves since that epoch, probably due to environmentally driven processes. Many processes can and have been imagined which could produce such population inhomogeneities in a natural manner. They include ram pressure stripping of the Galactic interstellar medium by the hot gas in clusters (Gunn & Gott 1972), tidal encounters between galaxies, mergers (Barnes & Hernquist 1991), the tidal effects of the cluster potential on galaxies (Byrd & Valtonen 1990), and disruption of a galaxy's external gas supply (Larson, Tinsley, & Caldwell 1980). Among others, this view has the virtue of economy of hypotheses, in that one process, the progressive depletion of gas-rich galaxies in populous environments, is responsible for both the present-

day morphology-environment relation and the observed evolution of cluster galaxies.

This, which we shall call the evolutionary hypothesis, is not, however, the only possible conclusion which one might draw. Dressler & Gunn (1983) have advanced a very different hypothesis: whether or not there has been significant evolution of most galaxies, in or out of clusters, the blue galaxies seen in high-redshift clusters are the result of other peculiar circumstances and are not representative of the general cluster population. Drawing upon the spectral peculiarities of many of the blue cluster members, which suggest the prevalence of starbursts, and upon their spatial and velocity distributions, Dressler and Gunn suggest that the blue galaxies are infalling objects undergoing a burst of *ram pressure–induced star formation* (RPISF). Models for the formation of clusters by Evrard (1990) predict the existence of a strong shock in the intracluster medium at earlier epochs, at radii of order 1 Mpc. Gas-rich field galaxies falling into a cluster for the first time will have their interstellar medium strongly shocked when they encounter this intracluster medium shock. A burst of star formation will be induced, after which the remaining gas will be swept from the galaxy. Evrard's models further predict that the strength of the shock will be much diminished by the present epoch, so that few starbursting galaxies are expected at $z = 0$.

The RPISF model, then, interprets the evolution in f_B in rich clusters as indicative not of the evolution of galaxies, per se, but of the evolution of clusters. The underlying morphology-environment relation of undisturbed galaxies might be unchanged with epoch. This is a radically different interpretation of Figures 16 and 19: the relation in Figure 16 characterizes all epochs; the higher values of f_B seen in rich systems in Figure 19 are due to interlopers, anomalous objects which have disappeared by the present epoch.

Unfortunately, each of the two hypotheses described above is consistent with the data we have presented in this paper. There is a suggestion, in a comparison of Figure 16 and Figure 19, of an evolution of f_B in systems with $1.3 < \log N_{0.5}^{-19} < 1.5$, which are probably too poor for ram pressure–induced star formation to occur, but the evidence is much too weak to be of use. Fortunately, the RPISF model makes very specific predictions, which may be tested with other available data.

In the RPISF model the blue galaxies are infallers and are on high-velocity radial orbits. Calculations by Evrard (1991) predict that they should have a velocity dispersion 70% higher than that of the other cluster members. At least 14 distant clusters containing blue galaxies now exist with substantial spectroscopic data. The velocity dispersions derived from these data are summarized in Table 7. We have divided the 399 cluster members with measured velocities into red and blue classes, using the criterion that blue galaxies are all those whose spectral energy distributions indicate the presence of some young population. The spectral characteristics of these blue galaxies range from that of ongoing starbursts to that indicating star formation several billion years in the past, but all should be, on the RPISF interpretation, members of the infalling population. The velocity dispersions in Table 7 have been calculated with respect to the mean velocity defined by *all* the cluster members, blue and red; any other approach would lead to a biased value.

The results show that the relative velocity dispersions for the blue and red members vary from cluster to cluster, but those of the blue members tends to be slightly higher. In each cluster, we form the ratio $\sigma_{\rm blue}/\sigma_{\rm red}$ and calculate means for all 14 clusters by a weighted sum, using $n_{\rm blue}$ and $n_{\rm red}$ as the weights. We find, for all 14 clusters, $\sigma_{\rm blue}/\sigma_{\rm red} = 1.21 \pm 0.09$. According to Evrard's models, this is much too low a ratio for an infalling population. It is, however, about what one might expect under the evolutionary hypothesis, in which population differences are caused by environmental effects. Such effects should be strongest in cluster cores. Galaxies whose orbits cause them to spend most time in the cluster core will evolve to the red faster than those which only venture occasionally into the core. If one measures the velocities of galaxies which are, at the time of observation, in the cluster cores, which is where all of the spectroscopic data has been obtained, one would expect the red galaxies to be more tightly bound and have lower velocity dispersions than the blue ones.

TABLE 7

RED AND BLUE RELATIVE VELOCITY DISPERSIONS

Cluster	z	$n_{\rm red}$	$n_{\rm blue}$	$\sigma_{\rm blue}/\sigma_{\rm red}$	References
Abell 963	0.206	8	11	1.27 ± 0.43	1
Abell 2111	0.229	6	10	1.06 ± 0.36	1
AC 103	0.309	26	10	1.07 ± 0.27	2
AC 114	0.317	29	13	1.38 ± 0.32	2
AC 118	0.307	26	8	1.14 ± 0.31	2
Cl 1358	0.327	47	7	1.55 ± 0.42	3
Cl 1447+2619	0.369	8	5	2.18 ± 0.78	4
Abell 370	0.373	19	30	0.85 ± 0.18	5
Cl 0024+1654	0.391	12	13	0.90 ± 0.25	6
Cl 0939+4713	0.407	21	8	0.51 ± 0.14	7
Cl 0303+1706	0.418	11	7	2.35 ± 0.75	7
3C 295	0.465	13	8	1.07 ± 0.32	7
Cl 1601+4253	0.539	17	9	1.89 ± 0.51	7
Cl 0016+1609	0.545	17	13	1.50 ± 0.38	7
All		260	152	1.21 ± 0.09	

REFERENCES.—(1) Lavery & Henry 1986; (2) Couch & Sharples 1987; (3) Fabricant et al. 1991; (4) Butcher & Oemler 1984b; (5) Soucail et al. 1989; (6) Dressler, Gunn, & Schneider 1985; (7) Dressler & Gunn 1991.

In the RPISF model one also expects a clear radial segregation in the spectral properties of the blue galaxies. The starbursts all occur in a well-defined region, the spherical shock located at about 1 Mpc radius. The shocked galaxies are all moving on radial orbits and, with infall velocities of order 2000 km s^{-1}, will reach the center in about 5×10^8 yr. This time is, coincidentally, about the same as the evolution time of the hot stars in the burst. One should, therefore, observe a steady radial progression in the age of the young population, with the youngest and bluest in a ring at ≈ 1 Mpc, and older and redder ones toward the center. Figure 20 presents the distribution of color versus radius of all spectroscopically confirmed cluster members in four clusters: Abell 370, Cl 0024+1654, Cl 1447+2619, and 3C 295. The red galaxies, those with $\Delta(B-V)_0 \lesssim 0.15$, are clearly more centrally concentrated than the blue ones. However, among the blue objects, there is no perceptible correlation of color with radius.

These results cast some doubt on the RPISF model, although they are not, in themselves, sufficient to rule it out, much less to establish that the evolutionary hypothesis is correct. Several kinds of observations suggest themselves as useful additions. For one, detailed observations of the blue galaxies in high-redshift groups and clusters can help establish the nature of these objects. The extant spectroscopy demonstrates that many of these galaxies have not had "normal" histories of star formation. Although ram pressure shocking of infalling galaxies is one method of producing such anomalies,

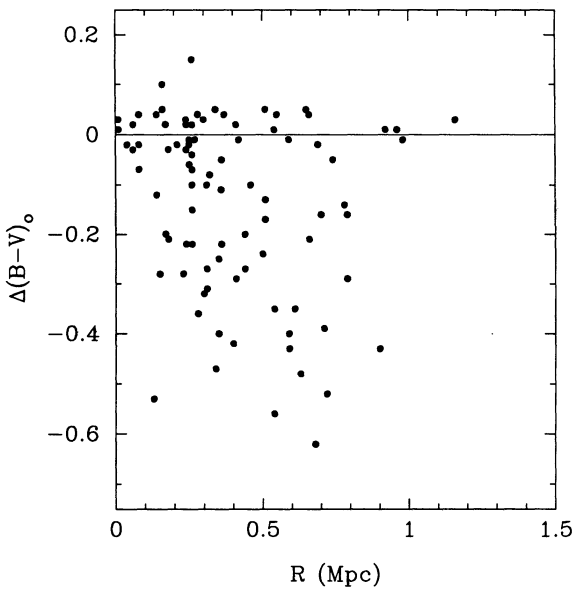

FIG. 20.—Distribution of $\Delta(B-V)_0$ vs. radius in four high-redshift clusters.

one can think of many more. Indeed, one can assert, after the fact, that such spectral peculiarities were to be expected. These galaxies exist under a set of conditions which does not occur today: gas-rich galaxies in regions of high density and high relative velocity. Given the potential for disturbance of the galactic interstellar medium which such conditions provide, it is not surprising that they have had unusual histories of star formation. Examination of their structure at high angular resolution may reveal characteristics indicative of particular types of interactions. For example, some observations already suggest that at least some of the blue galaxies are undergoing gravitational interactions (Lavery & Henry 1988, 1991).

Rich clusters were, apparently, the site of most rapid galaxy transformation at the epoch observed at $z = 0.4$. Figure 16 suggests that, at the present epoch, the corresponding environment, that at which the morphology-environment relation has the steepest gradient, is in rich groups or poor clusters. If the evolution of the morphology-environment relation has not run to completion, but continues today, rich groups are the site to search for evidence of the processes driving that evolution. One would equally like to explore conditions at yet earlier times. What would Figure 19 look like at $z = 1.0$? Does the flatness of the f_B versus N relation at $z = 0.4$ imply that little environmentally-driven evolution occurred before then? There is certainly room for some. The very centers of rich clusters are completely red even at $z = 0.4$. Are those residual differences the sign of primordial population variations, or only recent products of earlier evolution?

6. CONCLUSIONS

We have studied the evolution of galaxies in radio-selected groups for $z < 0.5$. We find the following:

1. By selecting groups according to the presence of a powerful radio galaxy, we avoid many of the redshift-dependent biases present in optical surveys.
2. Strong radio galaxies are found in a wide range of environments but not as wide as for groups in general.
3. There has been a slight decrease in the richness of radio-selected groups since $z = 0.4$, particularly for those containing radio galaxies of Fanaroff-Riley class II morphology.
4. The luminosity function of the members of the radio-selected groups is indistinguishable from that of field galaxies and does not appear to change over the redshift interval $0 < z \lesssim 0.5$.
5. Radio groups at low redshift ($z \sim 0.1$) display the same relationship between blue fraction and richness as is found in optically-selected groups.
6. At high redshift ($z \sim 0.4$) there is no evidence for such a trend: all groups have the same proportion of blue galaxies.

We conclude, therefore, that radio-selected groups are typical of groups in general and that the morphology-density relation is steepending with time. Thus rapid evolution in the colors of galaxies is seen only in rich clusters, indicating that the evolution is due to processes which are inefficient in poor environments.

We would like to thank Tom Broadhurst for his help in the early stages of this project. This work was partially supported by NATO grant 86/0514. A. O. and E. Z. were supported in part by grant AST-8722842 from the US National Science Foundation. We are grateful to the referee, Alan Dressler, for a number of helpful suggestions.

REFERENCES

Abell, G. O. 1958, ApJS, 3, 211
Allington-Smith, J. R., Spinrad, H., Djorgovski, S., & Leibert, J. 1988, MNRAS, 234, 1091
Babul, A., & Rees, M. 1991, in Clusters and Superclusters of Galaxies: Contributed Talks and Poster Papers, ed. M. M. Colless, A. Babul, A. C. Edge, R. M. Johnstone, & S. Raychaudhury (Cambridge: Institute of Astronomy), 85
Barnes, J. E., & Hernquist, L. E. 1991, ApJ, 370, L65
Barrow, J. D., Bhvasar, S. P., & Sonoda, D. H. 1984, MNRAS, 210, 19P
Benn, C. R., Grueff, G., Vigotti, M., & Wall, J. V. 1988, MNRAS, 230, 1
Broadhurst, T. J., Ellis R. S., & Glazebrook, K. 1992, Nature, 6355, 55
Broadhurst, T. J., Ellis, R. S., & Shanks, T. 1988, MNRAS, 235, 827
Bruzual, A., G., & Kron, R. G. 1980, ApJ, 241, 25
Burbidge, G., & Crowne, A. H. 1979, ApJS, 40, 583
Burstein, D., & Heiles, C. 1982, AJ, 89, 1165
Butcher, H. R., & Oemler, A. 1979, ApJ, 226, 559
———. 1984a, ApJ, 285, 426 (B&O)
———. 1984b, Nature, 310, 31
Byrd, G., & Valtonen, M. 1990, ApJ, 350, 89
Christian, C. A., Adams, M., Barnes, J. V., Butcher, H., Haynes, D. S., Mould, J. R., & Siegel, M. 1985, PASP, 97, 363
Colless, M., Ellis, R. S., Taylor, K., & Hook, R. N. 1990, MNRAS, 244, 408
Couch, W. J., & Sharples, R. M. 1987, MNRAS 229, 423
de Vaucouleurs, G., de Vaucouleurs, A., & Corwin, H. G. 1976, The Second Reference Catalogue of Bright Galaxies (Austin: Univ. of Texas Press) (RC2)
Dressler, A. 1978, ApJ, 223, 765
———. 1980, ApJ, 236, 251
Dressler, A., & Gunn, J. E. 1983, ApJ, 270, 7
———. 1991, ApJS, 78, 1
Dressler, A., Gunn, J. E., & Schneider, D. P. 1985, ApJ, 294, 70
Efstathiou, G., Ellis, R. S., & Peterson, B. 1988, MNRAS, 232, 431
Evrard, A. E. 1990, ApJ, 363, 349
———. 1991, MNRAS, 248, 8P
Fabricant, D. G., McClintock, J. E., & Bautz, M. W. 1991, ApJ, 381, 33
Fanaroff, B. L., & Riley, J. M. 1974, MNRAS, 167, 31P
Geller, M. J., & Huchra, J. P. 1983, ApJS, 52, 61
Graham, J. 1981, PASP, 93, 29
Guiderdoni, B., & Rocca-Volmerange, B. 1988, A&AS, 74, 185
Gunn, J. E., & Gott, J. R. 1972, ApJ, 176, 1
Hill, G. J., & Lilly, S. J. 1991, ApJ, 367, 1 (HOL)
Hubble, E. 1936, The Realm of the Nebulae (New Haven: Yale Univ. Press)
Kirshner, R. P., Oemler, A., Schechter, P. L., & Shectman, S. A. 1983, AJ, 88, 1285
Koo, D. 1981, ApJ, 251, L75
———. 1986, ApJ, 311, 651
Koo, D., Ellis, R. S., & Windhorst, R. 1989, private communication

Kristian, J., Sandage, A., & Westphal, J. A. 1978, ApJ, 221, 383
Kron, R. G. 1980, ApJS, 43, 305
Kron, R. G., Sprinrad, H., & King, I. R. 1977, ApJ, 217, 951
Laing, R. A., Riley, J. M., & Longair, M. S. 1983, MNRAS, 230, 1
Landolt, A. U. 1973, AJ, 78, 959
———. 1983, AJ, 88, 439
Larson, R. B., Tinsley, B. M., & Caldwell, C. N. 1980, ApJ, 237, 692
Lavery, R. J., & Henry, J. P. 1986, ApJ, 304, L5
———. 1988, ApJ, 330, 596
———. 1992, in Clusters and Superclusters of Galaxies, ed. A. C. Fabian (Dordrecht: Kluwer), in press
Lilly, S. J., Cowie, L. L., & Gardner, J. P. 1991, ApJ, 369, 79
Lilly, S. J., & Prestage, R. M. 1987, MNRAS, 225, 531
Molinari, E., Buzzoni, A., & Chincarini, G. 1990, MNRAS, 246, 576
Moore, B. E., Frenk, C. S., & White, S. D. M. 1992, private communication
Oemler, A. 1974, ApJ, 194, 1
———. 1992, in Clusters and Superclusters of Galaxies, ed. A. C. Fabian (Dordrecht: Kluwer) in press
Pence, W. 1976, ApJ, 203, 39
Perryman, M. A. C., Downes, A. J. B., & Lilly, S. J. 1985, MNRAS, 216, 641
Peterson, B., Ellis, R. S., Kibblewhite, E. J., Bridgeland, M. T., Hooley, T., & Horne, D. 1979, ApJ, 233, L109
Postman, M., & Geller, M. J. 1983, ApJ, 281, 95
Prestage, R. M., & Peacock, J. A. 1988, MNRAS, 230, 131; erratum 1989, MNRAS, 236, 959 (P&P)
Sandage, A. 1972a, ApJ, 178, 1
———. 1972b, ApJ, 178, 25
———. 1973a, ApJ, 183, 711
———. 1973b, ApJ, 183, 731
Sandage, A., Kristian, J., & Westphal, J. A. 1976, ApJ, 205, 688
Schechter, P. L. 1976, ApJ, 203, 297
Shane, C. D., & Wirtanen, C. A. 1967, Pub. Lick Obs., 22, Part 1
Shanks, T., Stevenson, P. R. F., Fong, R., & MacGillivray, H. T. 1984, MNRAS, 206, 767
Soucail, G., Mellier, Y., Fort, B., & Cailloux, M. 1988 A&AS, 73, 471
Sprinrad, H., Djorgovski, S., Marr, J., & Aguilar, L. 1985, PASP, 97, 932
Smith, E. D. 1989, ApJS, 69, 365
Tyson, J. A. 1988, AJ, 96, 1
Visvanathan, V., & Sandage, A. 1977, ApJ, 216, 214
West, M. J., Dekel, A., & Oemler, A. 1987, ApJ, 316, 1
West, M. H., Oemler, A., & Dekel, A. 1989, ApJ, 346, 539
Yates, M. G., Miller, L., & Peacock, J. A. 1989, MNRAS, 240, L129